Master Thesis
TVVR 22/5016

# Impact of Extreme River Flows on Bridges

## An Application to River Lagan in Ljungby Municipality, Sweden Using HEC RAS

Assad Mohammad Tahir

Division of Water Resources Engineering
Department of Building and Environmental Technology
Lund University

# Impact of Extreme River Flows on Bridges

## An Application to River Lagan in Ljungby Municipality, Sweden Using HEC RAS

By:
Assad Mohammad Tahir

Master Thesis

Division of Water Resources Engineering
Department of Building & Environmental Technology
Lund University
Box 118
221 00 Lund, Sweden

Water Resources Engineering
TVVR-22/5016
ISSN 1101-9824

Lund 2022
www.tvrl.lth.se

Master Thesis
Division of Water Resources Engineering
Department of Building & Environmental Technology
Lund University

| | |
|---|---|
| Swedish title: | Extrema flödens påverkan på broar. En studie av Lagan i Ljungby kommun med modellen HEC RAS. |
| English title: | Impact of Extreme River Flows on Bridges. An Application to River Lagan in Ljungby Municipality, Sweden Using HEC RAS. |
| Author: | Assad Mohammad Tahir |
| Supervisor: | Prof. Magnus Larson |
| Co-Supervisor: | Eng. Fainaz Inamdeen |
| Examiner: | Prof. Ronny Berndtsson |
| Language | English |
| Year: | 2022 |
| Keywords: | HEC RAS; Extreme River Flow; River Bridges; Ljungby; Lagan; Climate Change. |

Cover photo of Replösabron from Clemens Klante.

# Acknowledgements

Words cannot express my gratitude to Prof. Magnus Larson and Eng. Fainaz Inamdeen in the Division of Water Resources Engineering for providing me with the opportunity to work on this thesis study and for supervising me during my study.

I would also like to thank the Swedish Transport Administration (Trafikverket) and the Ljungby Municipality (Ljungby Kommun), especially Pontus Petersson and Tobias Wagner, for providing us with detailed drawings of the bridges, as well as bathymetric and water level data for the river.

It is also my privilege to thank all of my teachers, especially Dr. Ali Alzaed and Dr. Mamdooh Alwetaishi from Taif University, Saudi Arabia, for supporting me throughout the course of my studies and encouraging me to pursue my master's degree. Moreover, I would like to acknowledge Dr. Abdel Fattah Al Shahari for his guidance and advice in order to complete my studies.

Thank you, Emmanuel Chijioke Ekwu, for being one of the greatest friends and classmates during this educational journey. FRIENDS, I would like to thank each and every one of you for being a source of inspiration and optimism.

Lastly, I would like to extend my deepest gratitude to my parents, brothers and sisters, dear wife, and my lovely children (Nadia & Leith) for their support and encouragement throughout my studies; without you, I would not be the person I am today.

# Abstract

The role of bridges in the transportation network has become increasingly important as they ensure the smooth and safe passage of people and goods across rivers and other bodies of water. Flowing water impacts bridges over rivers primarily in two ways: (1) Hydrodynamic forces that directly impact the structure and (2) scouring at the pier and abutment, including contraction scour. The design principles for bridges in Sweden are relatively simplistic, including both impacting forces and local scour. Therefore, the purpose of this thesis is to examine the impact of extreme river flows on bridges, particularly in circumstances beyond the design flow, using as a case study Ljungby Municipality, Skåne. Ten bridges are located across 6 km of the Lagan River within the municipality area. Although applications are made regarding Swedish conditions, the work is primarily based on international literature and experiences. An overview of the literature on the impacts of extreme river flows on bridges was conducted, as well as an analysis of the most common equations that have been used to model these impacts. Several countries, including the United States and Australia, have studied this topic extensively and recommended design and analysis procedures. Additionally, corresponding Swedish techniques were reviewed. This was followed by evaluation of HEC RAS (1D - steady flow) model for its ability to simulate the impact of extreme flows on bridges, including scour predictions using the Froehlich equation. This resulted in inundation and flood hazard maps for the study area (Ljungby Municipality), as well as the determination of overflowed bridges. A 100-year event resulted in the overflowing of Ljungsätersbron. During the 200-year event, Ljungsätersbron and Söderbron overflowed. Also, abutment scour analyses have been performed for all bridges. Overall, the model provided a satisfactory estimation of the potential threats posed by scouring at bridges abutments during extreme flow conditions.

# 1 Introduction

## 1.1 Background

Bridges are crucial links in the transportation network that ensure smooth and safe passage over rivers and other water bodies. Damages to bridges causing reduced capacity, or even inoperability for transportation have severe economic and societal consequences (Kvočka et al., 2016). Also, the possibility for the rescue services to efficiently carry out its mission may be seriously affected. Thus, it is important to ensure that bridges perform satisfactorily under their lifespan in accordance with design conditions.

Bridges over rivers are primarily subjected to two types of impact from the flowing water: (1) forces from the water directly affecting the structure, including the possibility of overflow of the bridge at extreme conditions (Siregar, 2018); and (2) local erosion (scour) at and in the vicinity of the bridge, including pier, abutment, and contraction scour (Hung et al., 2017). The forces on the bridge are primarily determined by the flow velocity and the geometry of the bridge and water course, and whether any debris might be blocking the flow area, which often occurs during high-flow events. Bridge scour is also a function of similar variables, but in addition the properties of the bed and bank material are of significance as well as the geology at the site. Local scour is mainly due to flow contraction and secondary currents induced by the structure causing extra turbulence that generates increased sediment transport away from the structure.

In bridge design a flow has to be selected that the structure can withstand with regard to the impacts mentioned above, normally based on statistical analysis of measured or simulated flow time series at the location of interest. However, such time series might be rather short and form an uncertain basis for deriving design flows with sufficient accuracy. Also, with climate change, extreme events are expected to become more common and the design conditions that have been employed for existing bridges might underestimate future large flows (Yoon et al., 2019). Recent extreme flood events in Germany and Sweden indicate that some bridges may not be able to withstand future high flows. Thus, it would be highly useful to evaluate existing bridges for extreme flow events and to determine their response under such conditions.

In Sweden the design principles for bridges for local scour, are rather simplistic. Although the procedures in most previous cases have worked well, more advanced approaches would provide possibilities for efficient design and increased abilities of structures to function under extreme flow conditions (Honfi et al., 2018). Thus, developing approaches to analyze and design bridges for extreme conditions based on more detailed flow and impact evaluation, for example, using numerical models, would be of great value for all stakeholders involved in bridge construction, operation, and management.

## 1.2 Objectives

The overall objective of the present study is to determine the impact of extreme river flows on bridges, especially for conditions exceeding the design flow. Such situations may arise because the design flow estimates are not accurate (i.e., too low) or the flow conditions in the river has changed (e.g., due to climate change). The impact will be assessed with regard to direct flow effects, including overflow, as well as local scour. The possibility to describe the effects of debris on the flow conditions at bridges will also be investigated.

The study aims to accomplish the following objectives:

- A review of design procedures employed in different countries regarding impact of extreme flows on bridges.
- A description of expected impacts on bridges due to extreme flows, including direct forces (not the major focus of this thesis) and local scour.
- An investigation of approaches to model the impact, including procedures in the numerical model HEC RAS.
- An application of HEC RAS to the river Lagan in Ljungby to analyze the behavior of existing bridges during extreme flow events.
- An assessment of Swedish bridge design practices regarding extreme flows based on the case study in Ljungby.
- Inundation and flood hazard mapping for Ljungby Municipality under extreme river flows.

## 1.3 Methodology

The work was mainly based on international literature and experiences, although applications were made with regard to Swedish conditions. The work started with a literature review on the impacts of extreme river flows on bridges, particularly concerning forces on bridges during such events, also comprising overflow, and the development and effects of local scour. Different approaches to model these impacts were investigated and the most common equations identified. Design and analysis procedures recommended in a number of countries that have worked extensively on this topic (e.g., United States, and Australia) were examined. Also, corresponding Swedish procedures were reviewed and compared with other countries.

The HEC RAS simulation model were evaluated with regard to its ability to simulate the impact on bridges due to extreme flows. Of particular interest was approached to model overflow of bridges, although scour predictions were studied as well and the possibility to derive forces on the structure from flow simulations.

After the review of HEC RAS and its approaches to model extreme river flows and their impacts on bridges, the model was implemented for a stretch of the Lagan River at Ljungby. This stretch includes several bridges that historically have displayed vulnerability towards high flows. A statistical analysis was performed on available flow data to derive return periods for different magnitudes of flow. Based on this analysis, simulations with HEC RAS performed for 25-, 100-, and 200-years events (large flows) and the impact on the bridges was determined. The result was compared with the design conditions and an assessment made how well the bridges maybe impacted by extreme flow events.

## 1.4 Report Content

The thesis report is divided into eight chapters. The first chapter is "Introduction", in which general background, study objectives, current conditions in the study area, and significance of the study are discussed. Several basic mechanisms and theories of bridge scour including hydrodynamic forces impact, pier scour, contraction scour, and abutment scour are described in chapter 2 titled “Literature Review”. In addition, it provides information about available methods for estimating scour depth in the USA, Australia, and Sweden. A description of the study area is provided in Chapter 3, “Study Area”, including the river Lagan, the river bridges, and nearby existing scour conditions. A description of the theory of HEC RAS (1D - steady flow) is presented in chapter 4 “HEC RAS Model” by describing the essential functions and equations that are used to develop this model. In Chapter 5 “Model Implementation”, information about all input data are presented, such as DEM and bathymetry, details of bridge structures, boundary conditions, and flood frequency analysis. As described in Chapter 6 “Model Simulation”, calibration and validation of the model were performed, as well as simulated scenarios. Toward the end in Chapter 7 “Results and discussion”, we describe the results that extracted from this study, starting with flood inundation and hazard maps, identifying overflowed bridges, and assessing the potential scour risk of abutments. Eventually, the study was ended as described in Chapter 8 with a “conclusion and recommendations”.

## 1.5 Limitations

This study was subject to several limitations that may have affected the outcome. Obtaining the dimensions from old drawings for bridges was difficult (see Appendix II). Also drawings were missing for three bridges. When there were no drawings available for bridges, the elevations were extracted using SCALGO Live Tool. Furthermore, we could not perform pier and contraction scour analysis due to a lack of geotechnical data. In pier scour analyses, the D95 size fraction for the bed material is required, while the D50 (mean size fraction) and a water temperature are necessary for contraction scour analyses. Additionally, in our case, the flow data is only available over a limited time, i.e., 40 years, and cannot be used to estimate long return periods. Accordingly, we conducted scour analyses for 100 and 200-year events; however, performing scour analyses for 100 and 500-year events is recommended in the literature. Lastly, only one station is available in the middle of the study area for recording hourly water levels. The daily average of these data were used to calibrate and validate the model, resulting in high R2 values for both. The calibration of the model would be enhanced if water levels were recorded upstream and downstream of the study area. However, despite these limitations, the model achieved the study's objectives.

# 2 Literature Review

## 2.1 General

Extreme floods can directly cause deaths and property damages, including hydraulic structures when they are located on rivers. River bridges are very critical when they face sudden large flood waves and can ultimately lead to structure failure. The amount of flow and the water level of rivers rise dramatically during flooding. Dynamic conditions in bridge openings might change, pressured and weir flows might occur, and scouring around piers and abutments might cause deepening as a result of these significant changes. Due to possible climate change impacts throughout the world, the rainfall-runoff relationships, the flooding intensity, and frequency have varied in recent years. This may result in a greater risk to river bridges in term of hydraulic pressure. The structure of river bridges is quite complex, and they are located in a very dynamic environment. Many parameters are interacting with each other within the dynamic system. For example, flooding can occur due to a short but extremely heavy precipitation or sudden snow melt due to changes in weather, changes in rainfall-runoff relationships, and changes in runoff amounts due to varying in land cover or land use. Consequently, bridges in river environments are directly or indirectly affected by these factors. Hydraulic evaluation of river bridges has not been as extensively studied in the literature as it has been for structural evaluation (Koçyiğit et al., 2016). Generally, hydraulic factors are the primary cause of river bridge failure or damage. Flooding is one of the most destructive and important factors among these factors. In addition, riverbed degradation and scouring could also cause serious damage or even complete collapse of the bridge.

## 2.2 Overflowing Impact on Bridges

Due to the increased flow discharge during flooding, the water level rises significantly. As a result, during severe flooding, the water level can reach the lower girder of the bridge deck. When this happens, the flow is no longer free and rush through bridge opening, referred to as pressurized flow. The water level can even exceed the bridge deck due to further increases in stream discharge. Here, the bridge acts as a weir and the flow is of weir type and called weir flow. Under these circumstances, it may have a significant impact on sediment transport on riverbeds under bridge decks. Therefore, most river bridges fail due to excessive scouring around their piers when the flow is extremely high (Koçyiğit et al., 2016).

There was extensive damage to over 500 bridges in Georgia (USA) in 1994 as a result of tropical storm Alberto, which dumped 71 cm of rainfall over widespread areas of the state in a short period of time. Overtopping of bridges was a common cause of bridge damage after scour occurred around abutments and approach embankments (Parola et al., 1998). Overtopping caused extensive damage to bridge abutments and embankments in Georgia in 2009, with the flood recurrence interval exceeding 500 years (Gotvald and McCallum, 2010). There is a significant backwater effect created across a submerged bridge, including its deck and abutments, creating an indistinguishable and strongly varying water surface profile over the bridge deck and immediately downstream.

## 2.3 Hydrodynamic Forces on Bridge Decks

In flood events, river bridge decks are subjected to significant hydrodynamic loads if they are partially or entirely submerged. FHWA (Federal Highway Administration of the US) conducted a study in 2009 to determine the hydrodynamic forces on bridge decks under flood conditions. The study indicated that fluid properties and bridge configuration are important factors in determining the structural response of bridge decks (Figure 1). Although this thesis does not include calculations of hydrodynamic forces on bridge decks, it is important to briefly mention this input because it is essential to cover all aspects of the problem.

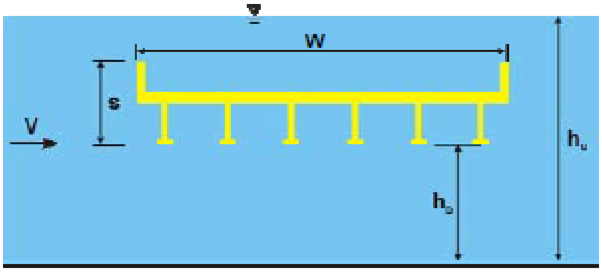


Figure 1. *A schematic of an overflowed river bridge* (FHWA, 2009).

A significant impact is exerted by the height and velocity of the water. Inundation ratio ($h^*$) is the height of the water surface with respect to river dimension, bridge deck position, and flow velocity. An inundation ratio is calculated using equation 1. It consists of the difference between free surface height over low chord height ($h_u$ - $h_b$) divided by deck thickness ($s$).

$$h^* = \frac{h_u - h_b}{s} \qquad (eq. 1)$$

The Froude number (Fr) provides a dimensionless measure of the flow velocity. It is calculated by dividing the free stream velocity, *v*, by the square root of the depth of flow, and by the gravitational acceleration, *g* in equation 2.

$$Fr = \frac{v}{\sqrt{gh_u}} \qquad (eq. 2)$$

As illustrated by Figure 2 below, an overflowed bridge deck is subjected to three primary forces. Bridge deck horizontal stability is affected by drag force ($F_D$), which acts parallel to flow and pushes on both piers and abutments. The lift force ($F_L$) allows the bridge deck to be lifted vertically and perpendicular to the flow from its piers and abutments. It is possible for bridges to overturn if heavy loads are unevenly distributed on the bridge decks, resulting in moments about the bridge's center of gravity ($M_{cg}$).

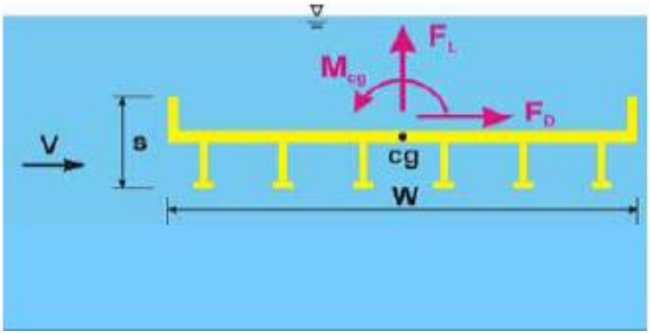


Figure 2. *An illustration of the forces acting on the bridge deck.* (FHWA, 2009).

Nondimensional coefficients are used to express forces such as drag and lift and moments that act on the bridge deck; equations 3a, 3b, 4 and 5 represent them, respectively, as shown below, where $\rho$ indicates the density of water, and $L$ indicates the length of the bridge.

$$C_D = \frac{F_D}{\frac{1}{2}\rho v^2 (Ls)} \quad (if\ h^* \geq 1) \qquad (eq. 3a)\ C_D - Drag\ coefficient$$

$$C_D = \frac{F_D}{\frac{1}{2}\rho v^2 [L(h_u - h_b)]} (if\ h^* \geq 1) \qquad (eq. 3b)\ C_D - Drag\ coefficient$$

$$C_L = \frac{F_L}{\frac{1}{2}\rho v^2 (LW)} \qquad (eq. 4)\ C_L - Lift\ coefficient$$

$$C_M = \frac{M_{cu}}{\frac{1}{2}\rho v^2 (LW^2)} \qquad (eq. 5)\ C_M - Moment\ coefficient$$

## 2.4 Effect of Debris

There is a potential for additional damage and danger when sediment or water borne debris are present in the floodwaters, such as vegetation, trunks of trees, and fence posts, which will only serve to enhance the impact of the floodwaters. Most of the time, large pieces of debris will move at approximately the same speed as the flow, and in this way, they turn into projectiles within the flow and become part of the flow itself. Bridges and other structures may also be impacted by heavy rafts of debris, increasing their load and the risk of collapse (Water Research Laboratory, 2015).

The depth and speed at which flood waters travel can be used to describe the force of flood waters. However, floodplains have different shapes and volumes of flow, which affects the speed and depth of flow in any particular local area. In extreme cases, underflow speeds can reach 75 km/h at the base of large dam spillways. It has been measured that river rapids flow at speeds of 22 km/h and in some cases, speeds have been reported as high as 55 km/h. In addition, flow over floodplains rarely experiences velocities exceeding 20 km/h (5.5 m/s), even in extreme situations (Water Research Laboratory, 2015).

During controlled tests, Chow (1959) found that flow speeds of 16 km/h (4.4 m/s) can erode rocks with a diameter of 0.2 m. The Main Roads Western Australian design guidelines found that 0.5 tons of rock remain in place during flow speeds of 16 km/h (4.5 m/s) and 4 tons of rock during flow speeds of 22 km/h (6.0 m/s).

## 2.5 Bridge Scour

Water flowing over piers and abutments of bridges causes scour when it excavates and carries away material from the area around the bridges. Increasing precipitation frequencies and/or intensities may increase flows and scour rate at many locations in the near future (IPCC, 2013; Nasr et al., 2022). Several rivers in Sweden have recently been surveyed in detail with regard to their bathymetry. Cases have been reported where distinct scouring holes were found in the vicinity of bridges, providing evidence that this is a common problem (Das et al., 2021). River bridges are typically affected by three types of scour:

### *Local Scour*

Local scour refers to the removal of sediment from around bridge piers or abutments. Scour holes are created when water flows past a pier or abutment. As an essential parameter for a detailed investigation of local scour, sediment properties and riverbed conditions should also be taken into account when constructing proper countermeasures to prevent erosion, slides, and structural damage. Bridges commonly collapse due to scour at their foundations, which include piers and abutments. Richardson et al. (1993) studied 383 bridge failures in the USA and concluded that 25% of the damages were caused by pier scour, and 72% by abutment scour (Das et al., 2021).

### *Contraction Scour*

As the flow cross-section of a river changes, sediment is removed from the bottom and sides of the river by contraction scour. Water moves faster through narrower bridge openings, resulting in transport gradients and contraction scour.

### *Degradational scour*

Scouring by degradation is the process of general removal of sediment from the bottom of a river by its flow. There is no correlation between the presence of a bridge and this type of sediment removal, the general erosion causing consistent lowering of the river bottom, but over time, a large amount of sediment may be removed. Figure 3 illustrates the different types of scour that occur on a bridge.

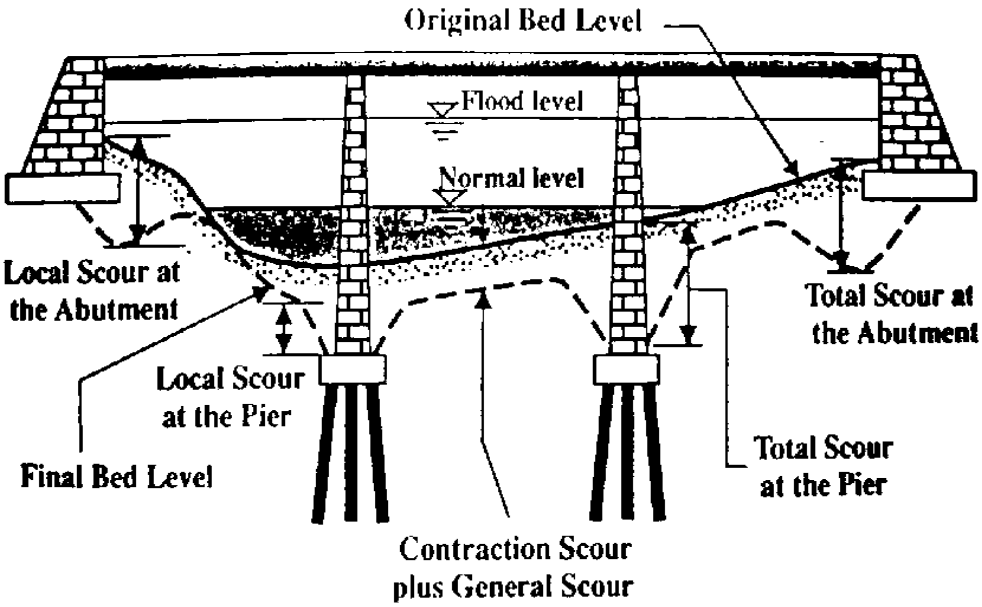


Figure 3. *A schematic diagram showing the types of scour that may occur near a bridge site* (Melville and Coleman, 2000).

## 2.6 River Bridge Failures in Sweden

According to Inamdeen (2020), Sweden has a lack of detailed investigation of bridge scour to quantify the extent of the damage it causes to bridges as a result of local scour. However, some bridge failures due to scour have been documented. As an example one of the bridge piers failed during the final stage of the bridge construction across the Österdal River in 1979 after high flow scoured it (about 500 km west of Stockholm). Due to the extension of the abutments, the effective flow area was reduced by just under 40%; the scour protection was insufficient and did not meet the recommendations, and the sheet piles around the pier during construction increased the surfaces exposed to flow (Das et al., 2021).

Another example of failure due to scour occurred in 1973, where ice jamming caused serious damage to the bridge over the Lainio River in the most northern part of Sweden. As a result of the scouring of the riverbed, the bridge's middle pier settled by approximately 1.7 m. Since the native sediment was considered to be sufficiently stable, no special scour protection was placed around the bridge. After the damage, an inspection of the riverbed revealed a depth change of 3 m near the western abutment, which protrudes into the water significantly. There was a large, but not extreme, flow during the event resulting in the scour (Das et al., 2021).

## 2.7 International and Swedish Design Procedures

To protect bridges within the design life of the bridge, it is necessary to evaluate the risks associated with bridge scour. Generally, the procedures and steps for bridge scour analysis vary from country to country; however, they share many similarities. Moreover, increasing climate change effects associated with large river flows would enhance the importance of bridge scour evaluation at a detailed level (Das et al., 2021). The following are recommendations from a number of countries with extensive experience in this area (the United States, and Australia). A review and comparison of the corresponding Swedish procedures with those of the other countries was also conducted.

### 2.7.1 The United States (USA) - HEC 18 Method

HEC 18 provides proper guidance for comprehensive bridge scour evaluations issued by the Federal Highway Administration (FHWA). To produce a better hydraulic design, HEC 18 has the ability to estimate the total potential scour and evaluate the bridge foundation for scour risk. The total potential scour can be estimated by following a four steps procedure:

i. **Determining the scour design flood**
   It is important that the scour design flood is always greater than the corresponding hydraulic design flood as shown in table 1, in order to prevent bridge failures.

| Hydraulic Design Flood Frequency | Scour Design Flood Frequency |
|---|---|
| Q10 | Q25 |
| Q25 | Q50 |
| Q50 | Q100 |
| Q100 | Q200 |

Table 1. *Scour design flood with corresponding hydraulic design flood* (Arneson et al, 2012).

**ii. Developing hydraulic characteristics**

A model can be used to determine water depth, flow width, and velocity corresponding to scour design floods. As with HEC 18, HEC RAS software comes with a built-in bridge scour analysis option.

**iii. Estimating the total potential scour**

As a result of the two preceding steps (i and ii), the developed hydraulic conditions can be used to estimate the total potential scour. A combination of hydraulic, geotechnical, and structural data is required to determine:

- Longterm degradation or aggregation.
- Potential contraction, and local scour depth (pier, abutment).
- Foundation depth for abutments.

***Estimating contraction scour with HEC 18***

For non-cohesive soils, contraction scour can be estimated using the live-bed and clear water equations (6, and 7), respectively; equation 7 is an updated version of the Laursen (1960, 1963) formula according to Das et al. (2021).

$$d_s = \left(\frac{Q_2}{Q_1}\right)^{\frac{6}{7}} \left(\frac{W_1}{W_2}\right)^{k_1} y_o - y_{co} \quad (eq. 6)$$

| **Symbol** | **Description** |
|---|---|
| $d_s$ | Depth of equilibrium scour |
| $Q_1$ | The flow rate in the upstream channel transporting sediments, (m3/s). |
| $Q_2$ | The flow rate in the contracted channel, (m3/s). |
| $y_o$ | Depth of flow in a normal channel |
| $y_{co}$ | Depth of flow in the contraction zone |
| $W_1$ | Width of the bottom of the upstream main channel that transports bed material (m). |
| $W_2$ | The bottom width of the main channel in a contracted section minus the width of the piers (m). |
| $k_1$ | Exponent for mode of bed material transport (calculated from table 2 below) |
| $V*$ | Upstream approach section shear velocity (m/s). |
| ω | Bed material fall velocity based on temperature (T) and D50. According to the table 2 and Figure 4 below. |

| $V*/\omega$ | $K_1$ | Mode of Bed material transport |
|---|---|---|
| $< 0.50$ | 0.59 | Mostly contact bed material discharge |
| $0.50\ to\ 2.0$ | 0.64 | Some suspended bed material discharge |
| $> 2.0$ | 0.69 | Mostly suspended bed material discharge |

Table 2. *A coefficient indicating the mode of transport of bed material* (Das et al., 2021).

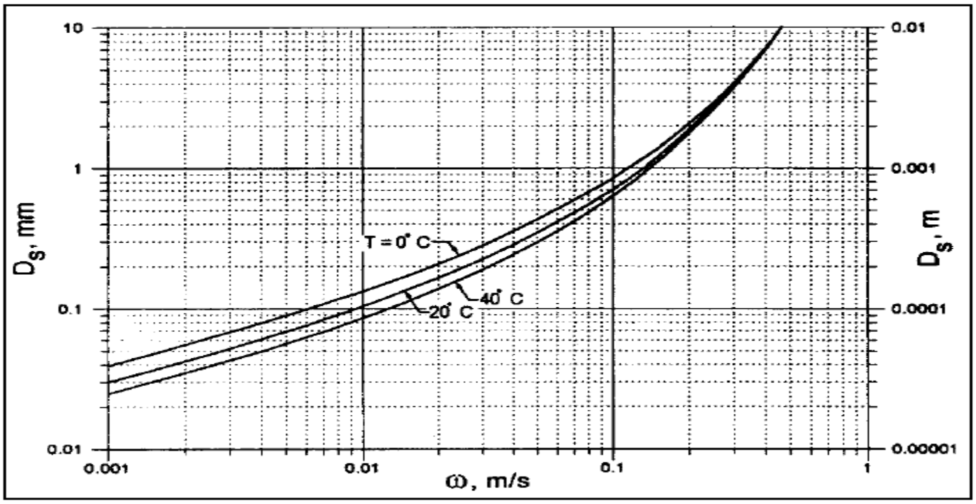


Figure 4. *The relationship between the fall velocity of sand-size particles and the temperature of the water* (Arneson et al., 2012).

According to Laursen (1963), the modified formula for clear-water scour is as follow:

$$d_s = \left(\frac{K_u\, Q_2^2}{D_m^{2/3}\, W_2^2}\right)^{\frac{3}{7}} - y_{co} \quad (eq. 7)$$

| | |
|---|---|
| $D_m$ | The diameter of the smallest, non-transportable particle within the contracting section (1.25 x D50). |
| $D_{50}$ | Bed material's median diameter (m). |
| $K_u$ | For metric units, use 0.025. |

In cohesive soils, the contraction scour can be estimated using the Briaud et al. (2011) equation 8.

$$d_s = 0.94\, y_o \left(\frac{1.83 U_{co}}{\sqrt{g y_o}}\right) - \frac{\sqrt{\frac{\tau_c}{\rho_w}}}{g n y_o^{1/3}} \quad (eq.\ 8)$$

| | |
|---|---|
| $\tau_c$ | The critical shear stress (N/m$^2$) |
| $n$ | The value of Manning. |
| $\rho_w$ | Water density (kg/m$^3$). |
| $U_{co}$ | Flow velocity in contraction zone |

***Estimating pier scour with HEC 18***

For non-cohesive soils, pier scour can be estimated using HEC 18 pier equation for both live-bed and clear water conditions (equation 9).

$$y_s = 2\ K_1 K_2 K_3\ g^{-0.125} y_o^{0.135} b^{0.65} V_o^{0.43} \qquad (eq. 9)$$

In cohesive soils, the pier scour can be estimated using the Briaud et al. (2011) equation 10.

$$y_s = 2.2\ K_1 K_2 b^{0.65} \left(\frac{2.6V_o - V_c}{\sqrt{g}}\right)^{0.7} \qquad (eq. 10)$$

| | |
|---|---|
| $g$ | Gravity acceleration |
| $y_s$ | Depth of scour (m) |
| $y_o$ | Approach depth (m) |
| $b$ | Pier width (m) |
| $V_o$ | Approach velocity (m/s) |
| $V_c$ | Critical velocity for the D50 size particle. |
| $K_1$ | Coefficient 1.1 based on the shape of the pier nose |
| $K_2$ | In order to correct for the skew of the pier to the approach flow, we derived an equation consisting of (cos α + (L/b) sin α) 0.65. |
| $K_3$ | The channel bed condition is corrected with a coefficient defined as 1.1, except when medium to large dunes are present. |

***Estimating abutment scour with HEC 18***

In order to estimate abutment scour, the Froehlich live-bed equation (equation 11) or the HIRE equation (equation 12) are used, as outlined below.

$$\frac{y_s}{y_o} = 2.27\ K_s K_\theta \left(\frac{1}{y_o}\right)^{0.43} F_o^{0.61} + 1 \quad (eq.11)\ Froehlich\ live - bed$$

$$\frac{y_s}{y_o} = 7.27\ K_s K_\theta\ F_o^{0.33} + 1 \quad (eq.12)\ \ HIRE$$

| | |
|---|---|
| $y_s$ | The maximum depth of clear-water equilibrium scour |
| $y_o$ | Approach depth (m) |
| $F_o$ | Froude number of flow |
| $K_s$ | Shape factor for abutments |
| $K_\theta$ | Alignment factor for abutments |

**iv. Plotting scour depths.**

Eventually, a cross-section of the channel and flood plain will be plotted to evaluate the estimated and adjusted scour depths in step iii, as well as to be utilized in the design of foundations. FHWA states that the above steps can also be used to evaluate the scour of existing bridges (Das et al., 2021).

### 2.7.2 The United States (USA) - Other methods

According to Das et al. (2021) for certain applications in the USA, there are a few other methods for estimating scour:

- *SRICOS-EFA Method*
  Scour Rate in Cohesive Soil-Erosion Function Apparatus; this method has the major advantage of including time effects and thereby estimating scour rates.

- *Simplified SRICOS Method*
  This simplified method relies on pre-classified charts to determine the characteristics of the soil and the erodibility of a particular site.

- *FDOT Method*
  Florida Department of Transportation developed this method for estimating pier scour in 2005.

- *ABSCOUR Method*
  This method is based on Maryland State Highway Administration (MDSHA) proposed equations for estimating abutment scour.

The reader is referred to Das et al. (2021) for more details.

### 2.7.3 Australia - Austroads scour guide (2019)

Bridge scour design procedures are described in "Guide to Bridge Technology Part 8: Hydraulic Design of Waterway Structures." It should be noted that the bridge scour design procedures are similar in most aspects to those described in HEC 18 of the Federal Highway Administration, USA. Nevertheless, the differences between the Austroads scour guide and the HEC 18 scour manual will be reviewed.

Foundations for new bridges are designed based on hydraulic design flood scour estimates. A 2000-year flood should also be considered when evaluating the designed foundation as an Ultimate Limit State (ULS). It is recommended that, if an overtopping flood condition exists and it is less than the 2000-year return flood, the overtopping flood will be taken into consideration for the evaluation of the foundation design without considering the ULS. Further, in order to determine the hydraulic characteristics for applicable flood scenarios, one- or two-dimensional hydraulic models can be used (Das et al., 2021).

### 2.7.4 Australia - Bridge Scour Manual of Queensland Department of Transport and Main Roads

A revised bridge scour manual has been published by the Department of Transport and Main Roads of the State of Queensland in January 2019. In 2018, Austroads released the bridge scour guide, edition 2.0. This document supplements that guide. Nevertheless, the majority of the additions and modifications relate to the HEC 18 scour manual. A two-dimensional model needs to be used in order to obtain hydraulic characteristics, as is acknowledged in the supplement guide. In addition, a preliminary assessment should be conducted to evaluate the field conditions surrounding the bridge site prior to estimating the depth of scour. As illustrated in Figure 5, an overview of the recommended procedure for conducting an in-depth scour assessment is provided.

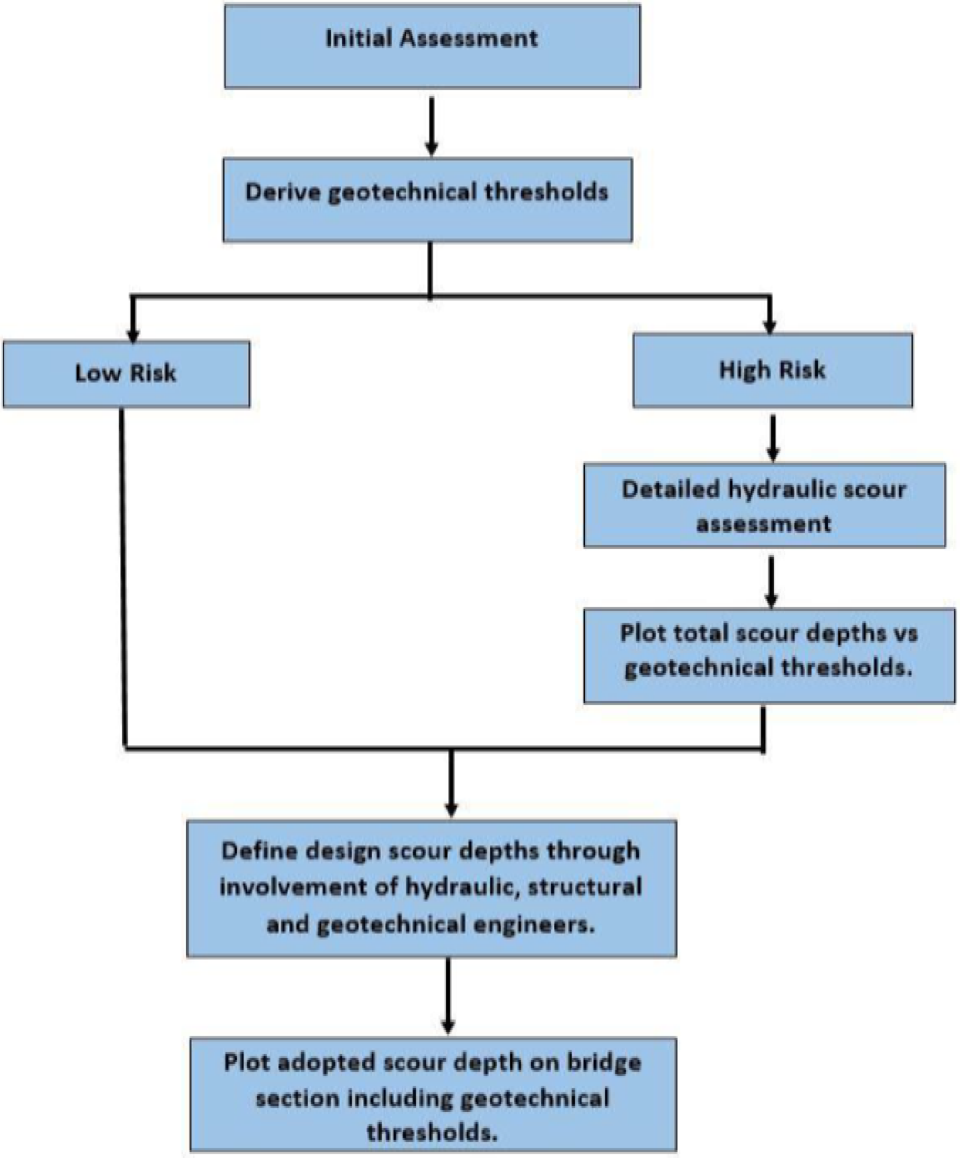


Figure 5. *An overview of the recommended methodology for scour assessment in the Queensland bridge scour manual* (2019).

### 2.7.5 Sweden

Currently, there is insufficient knowledge about bridge scour in Sweden, and no significant research has been carried out in recent years. According to the Swedish Transport Administration (Trafikverket) handbook, erosion protection for bridges has generally been designed with a margin of safety based on the average water velocity at flows corresponding to a return period of about 50 to 100 years, depending, for example, on the span of the bridge. A safety margin must include both locally higher water velocities particularly at bridge piers and abutments (Karlsson and Gunnarsson, 2017)

In the 1980s, the Swedish Road Administration (Vägverket) developed the current Swedish guidelines for scour analysis and design, available in Swedish (Erosionsskydd i Vatten vid väg – och Brobyggnad, 1987). However, the Swedish guidelines are not as detailed as those from other countries and are rather brief. Furthermore, Vägverket (1987) discusses only pier scour in its estimation of bridge scour, without addressing contraction or abutment scour.

***Pier Scour***

For pier scour, the applied method is identical to that suggested by the Laursen formula (equation 13), even though some coefficient values are presented graphically. Figure 6 shows a local scour depth ($Z_{max}$) in a pier; where, *y* is the water depth, *B* is the pier width, *L* is the length of the pier, and the *pier shape* should be also defined such as circular or rectangular.

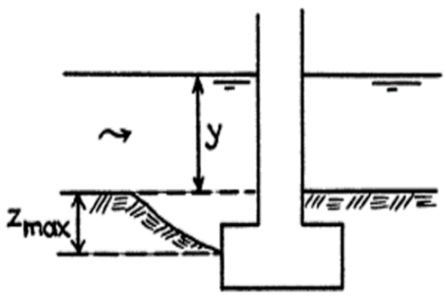


Figure 6. *Local scour at a pier* (Vägverket 1987).

$$Z_{max} = Z_e \, . \, k_\alpha \, . \, k_n \qquad (eq. 13) \;\; The\ Laursen\ Formula$$

| | |
|---|---|
| $Z_{max}$ | Depth of scour (m) |
| $Z_e$ | Depth of erosion in a rectangular pier of a bridge; obtaine in dimensionless form in Figure 7. $Z_e$/B as function of y/B |
| $k_\alpha$ | Coefficient depends on the pier length L and the angle (a) between the longitudinal axis of the pier and the flow direction. See Figure 8. |
| $k_n$ | Coefficient depends on pier shape. See Figure 9. |

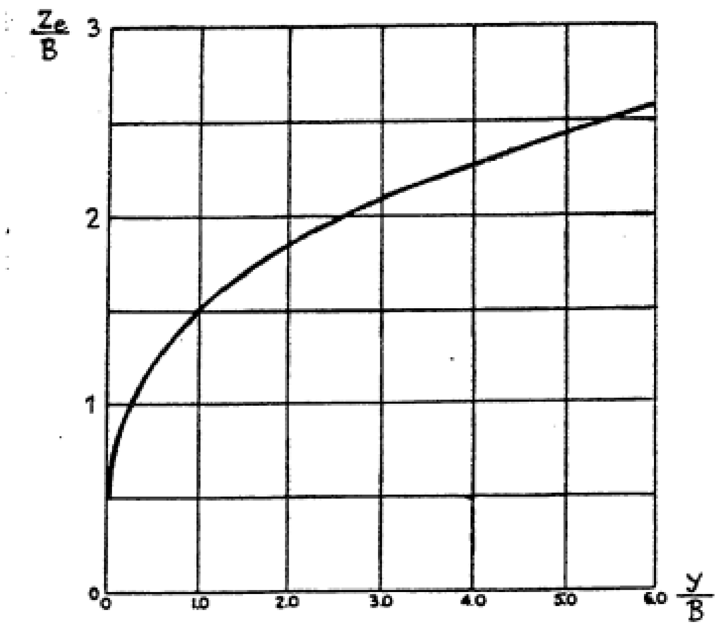


Figure 7. *Ze/B as function of y/B* (Vägverket 1987).

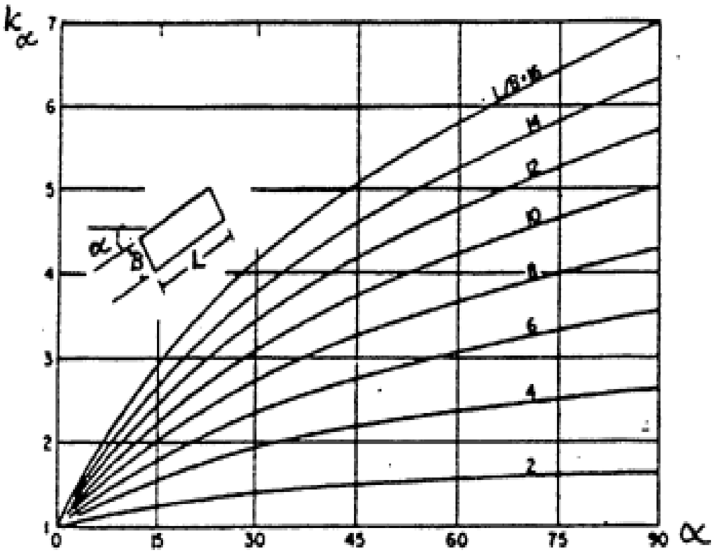


Figure 8. $K_\alpha$ *as function of α and L/B* (Vägverket 1987).

| Pier Shape<br>Shape | L : W | $k_n$ |
|---|---|---|
| Rectangular | — | 1,00 |
| Semicircula | 1:2 | 0,90 |
| Elliptical | 2:1<br>3:1 | 0,80<br>0,75 |
| Lens-shaped | 2:1<br>3:1 | 0,80<br>0,70 |

Figure 9. $K_n$ *as function of the pier shape* (Vägverket 1987).

# 3 Study Area

## 3.1 General

The Lagan River catchment is located in the southwestern part of Sweden, (Figure 10). Lagan River and its tributaries drain a total area of 6 445 $km^2$ along a 244 km path from Tahesjön in the north to Fagerhultasjön in the south, before entering Kattegat at Snapparp coast. Agricultural land dominates the southwestern regions of the catchment area, whereas mixed coniferous forests dominate the northeast. Ljungby Municipality covers approximately 22.5 percent of the entire catchment area and lies approximately halfway between the starting point of the river and the sea outlet (Bjerkén et la., 2021).

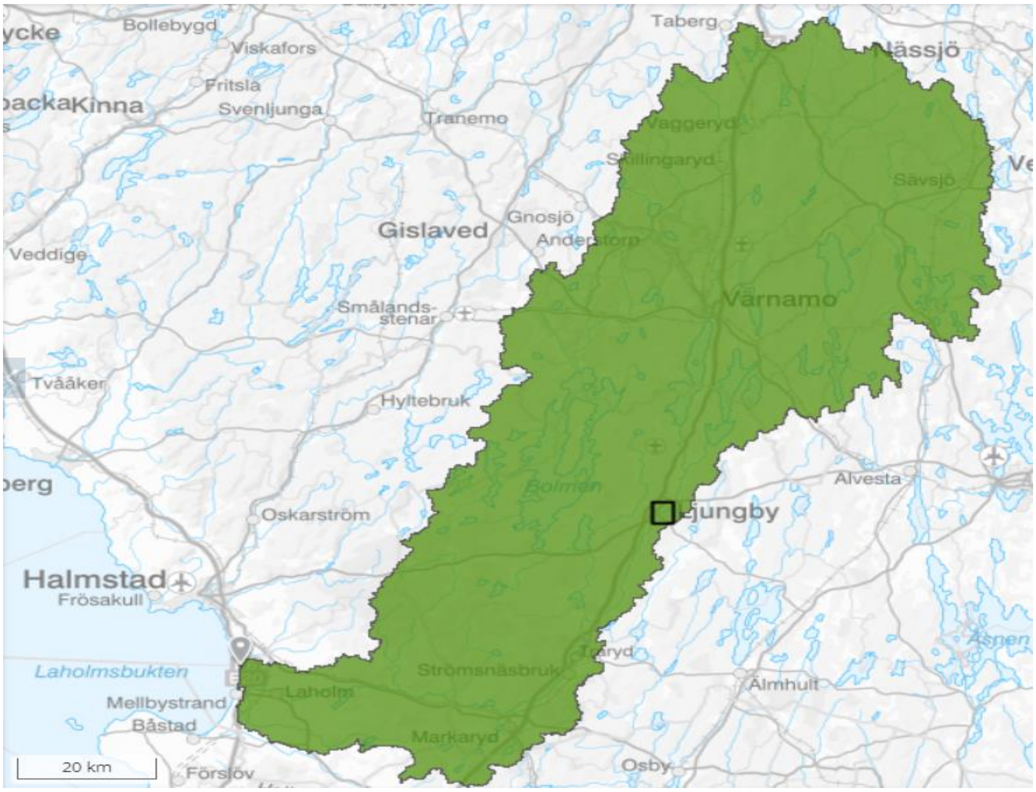


Figure 10. *Lagan River Catchment* (SCALGO Live).

## 3.2 River Bridges in Ljungby

There are ten river bridges located in the study area; Table 3 contains their names and the availability of bridge drawings, and Figure 11 shows their names and locations in the satellite image of Ljungby Municipality. In addition, a hydropower dam is also located upstream to Elverketsbron Bridge.

| | **Bridge Name** | **Drawings Availability** |
|---|---|---|
| 1 | Sickingebron (Trafikverket) | Yes |
| 2 | Replösabron | No |
| 3 | Ågårdsbron | Yes |
| 4 | Järnvägsbron | Yes |
| 5 | Tomtebobrön | Yes |
| 6 | Elverksbron | Yes |
| 7 | Ljungsätersbron | No |
| 8 | Industribron | Yes |
| 9 | Gängesbron | Yes |
| 10 | Söderbron | No |

Table 3. *River bridges in Ljungby Municipality*.

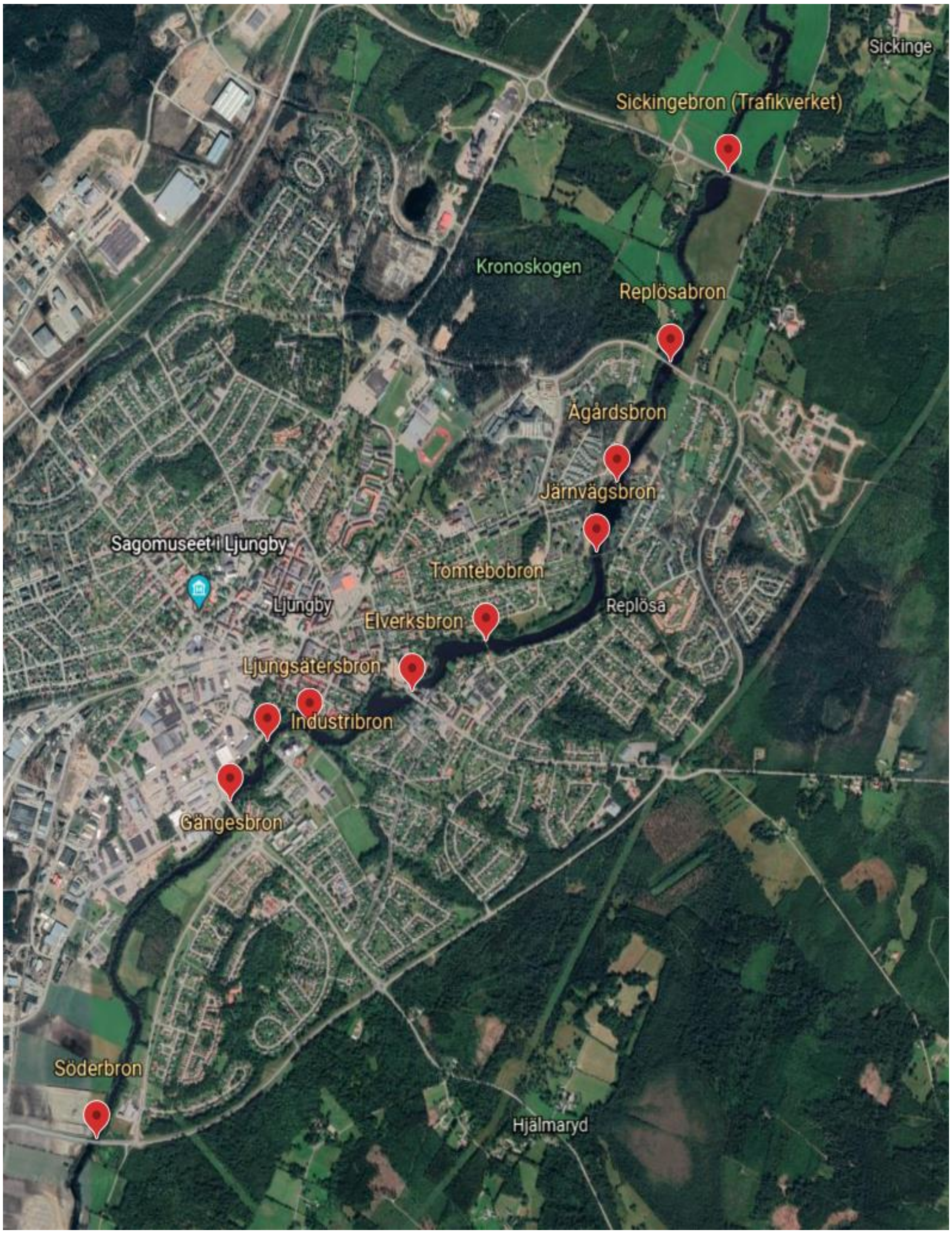


Figure 11. *River bridges at Ljungby Municipality.*

## 3.3 Bridge scour in Lagan, Ljungby

According to Ljungby Municipality, erosion has been observed along the riverbanks of Lagan (Figure 12 below). In addition, Das et al. (2021) mentioned local scour holes observed downstream of the two northernmost bridges Sickingebron and Replösabron. Scour holes have formed most likely due to contraction scour caused by the bridges.

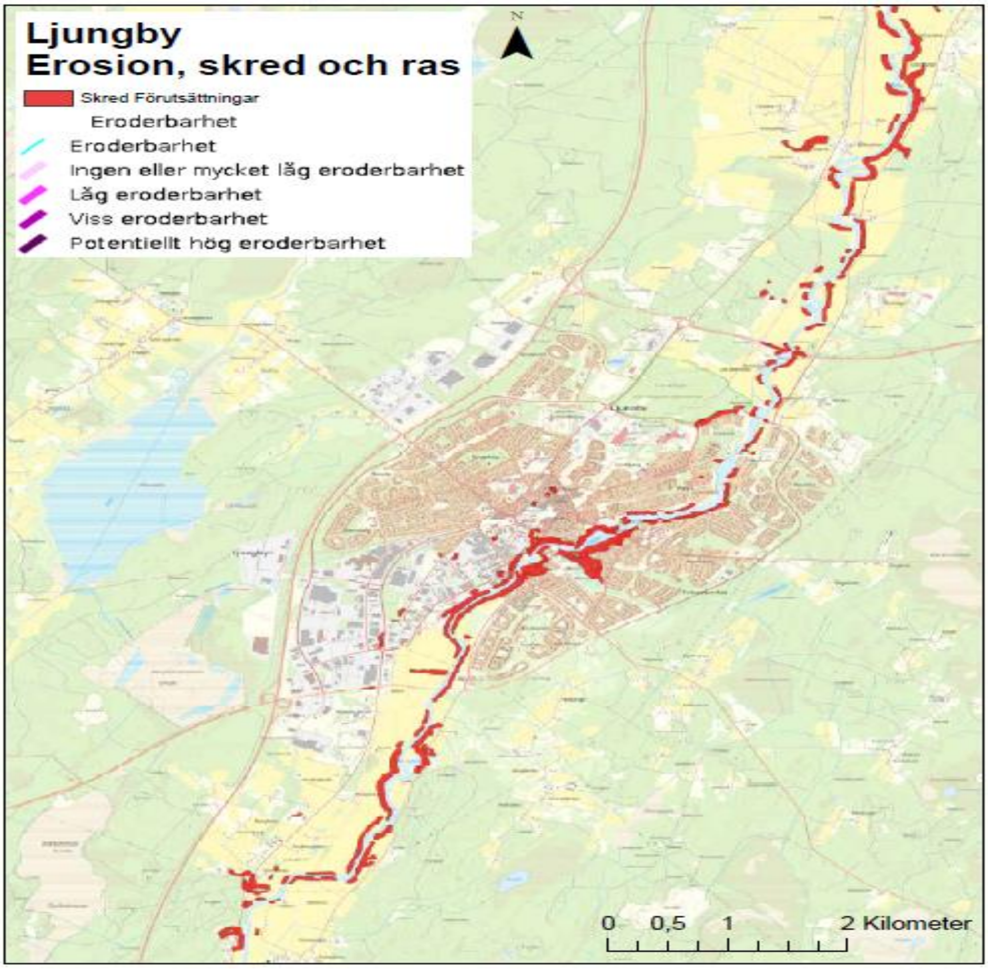


Figure 12. *Observed erosion along the riverbanks of Lagan in RED.* (Ljungby Kommun, 2022).

### ***Sickingebron Bridge***

The scour hole at Sickingebron is approximately 6 m deep from the undisturbed riverbed, and it is about 30 m wide and 50 m long. Bend effects may also be significant, affecting the flow direction through the bridge, resulting in an asymmetrical scour hole (see Figure 13).

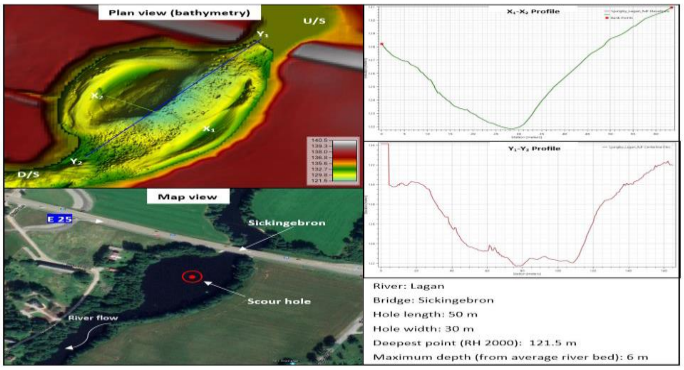


Figure 13. *A bathymetric map showing a scour hole downstream of the Sickingebron* (Das et al., 2021).

### ***Replösabron Bridge***

The scour hole downstream of Replösabron measures 2.5 m in depth, 30 m in width and 40 m in length. Geotechnical information at the sites was limited, therefore it was not possible to assess how these properties may influence the development of scour holes (see Figure 14).

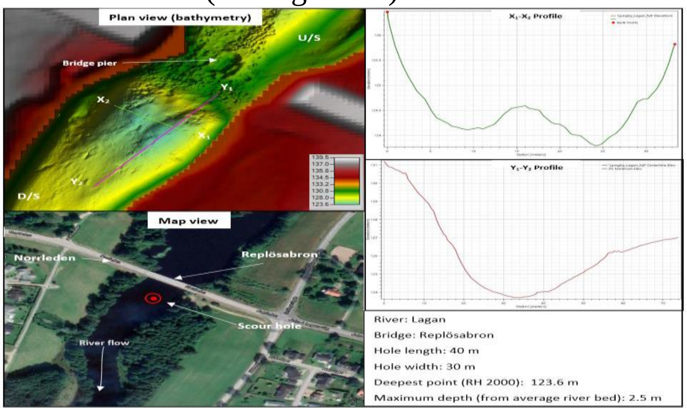


Figure 14. *A bathymetric map showing scour hole downstream Replösabron* (Das et al., 2021).

## 3.4 River Flow Data at Ljungby

Figure 15 illustrates the river flow from 1981 to 2021 based on data provided by the Swedish Meteorological and Hydrological Institute (SMHI). SMHI developed the Hydrological Predictions for the Environment (HYPE) model to simulate the flow of water and the flux of substances from precipitation to sea through different storage compartments (Lindström et al., 2010), HYPE is a semi-distributed catchment model that use a daily time step (SMHI, 2020). A Flood Frequency Analysis (FFA) was performed based on these data.

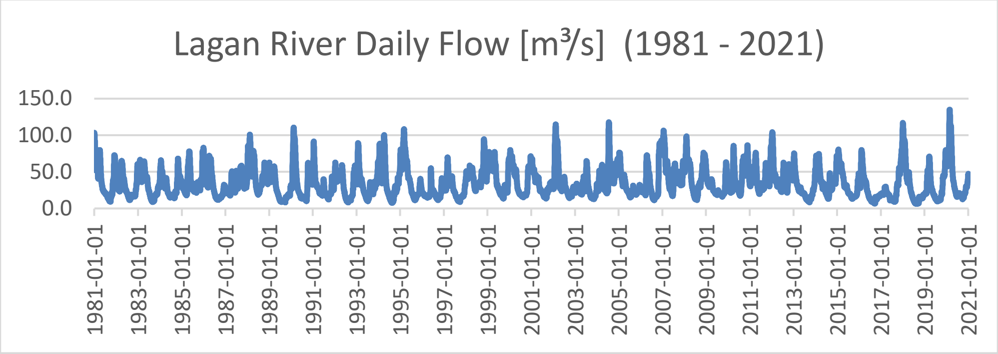


Figure 15. *Simulated daily river flow* (1981 - 2021).

Between 01/06/2018 and 12/04/2021, Ljungby Municipality provided hourly water level measurements at a point located below the Gängesbron. In order to calibrate and validate the model, we will use a daily average of these data (Figure 16).

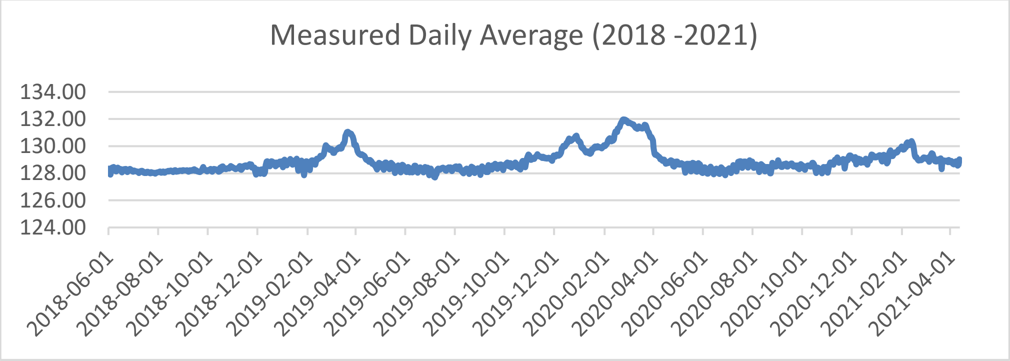


Figure 16. *Measured daily river water level* (2018 - 2021).

# 4 HEC RAS Model

## 4.1 General

The Hydrologic Engineering Center's River Analysis System (HEC RAS) is a tool developed for analyzing the river system's hydraulics by the United States Army Corps of Engineers (USACE). HEC RAS is freely available for users to encourage analysis of river hydraulics and better water management. One-dimensional (1D) steady flow, one-dimensional (1D) and two-dimensional (2D) unsteady flow, sediment transport, and water quality analysis can be done using HEC RAS (Brunner, 2021). A 1D hydraulic method gives good results in cases of flood propagation along the main river, as in the study area (Md Ali et al., 2015; Huţanu et al., 2020). Therefore, HEC RAS is considered a suitable modeling software for this study. A (1D) steady flow analysis was conducted to be sufficient in this study using HEC RAS version 6.1. The following is a brief review of the theoretical basis of what has been implemented in this thesis work, which involves (1D) steady flow, structures such as (bridges and dams), different boundary conditions, flood hazard mapping, and local scour calculations at abutments within the HEC RAS.

## 4.2 One Dimensional (1D) Steady Flow

HEC RAS is capable to perform one-dimensional water surface profile calculations for steady gradually varied flow. Steady flow is defined as a flow in which various parameters such as velocity, pressure, and flow density do not change over time at any given place. The surface profile is computed by solving the energy equation (equation 14) from one cross section to the next with standard step method. Figure 17 below, shows the energy equation terms.

$$Z_2 + Y_2 + \frac{a_2 V_2^2}{2g} = Z_1 + Y_1 + \frac{a_1 V_1^2}{2g} + he \qquad (eq. 14)$$

| | |
|---|---|
| $Z_1, Z_2$ | elevation of the main channel inverts |
| $Y_1, Y_2$ | depth of water at cross sections |
| $V_1, V_2$ | average velocities (total discharge/ total flow area) |
| $a_1, a_2$ | velocity weighting coefficients |
| $g$ | gravitational acceleration |
| $he$ | energy head loss |

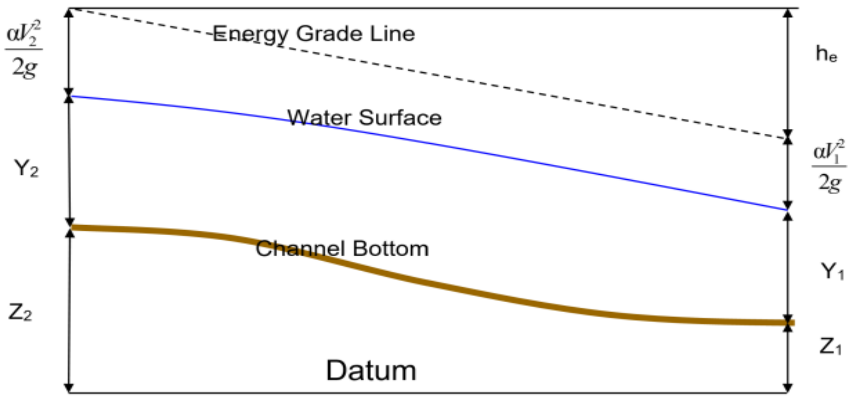


Figure 17. *Energy loss representation between two points* (Brunner, 2021).

When performing a (1D) steady flow analysis, each cross-section input is divided into three parts separated by a given Manning's value: the Left Over Bank (LOB), the Main Channel (Ch.), and the Right Over Bank (ROB), as shown in Figure 18 below. Then, iteratively solves the energy equation (Eq.14) using the standard step method to calculate the water level in all three of these subdivisions. Since HEC RAS assumes that the energy head is the same over the entire cross section and that water flows at right angles to it, the final energy of the cross section is the average of these energy levels (Brunner, 2021).

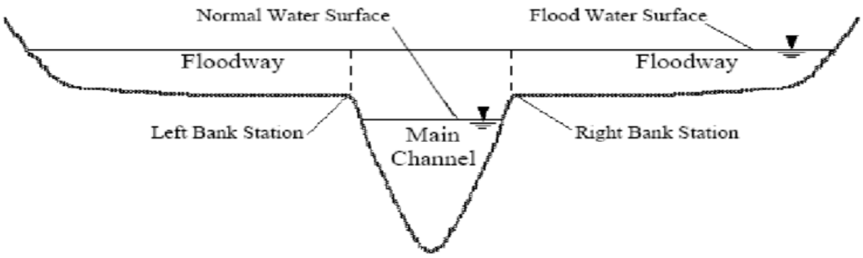


Figure 18. *An example of a stream cross section* (Tate, 1999).

Between two cross sections, the energy head loss *he* represents the friction losses and contraction, or expansion losses as shown in (equation 15).

$$he = L\overline{S_f} + C\left|\frac{a_2V_2^2}{2g} - \frac{a_1V_1^2}{2g}\right| \qquad (eq. 15)$$

| | |
|---|---|
| $\overline{S_f}$ | representative friction slope between two sections |
| $C$ | expansion or contraction loss coefficient |
| $L$ | discharge weighted reach length |

The distance weighted reach length ($L$) calculated as shown below (equation 16).

$$L = \frac{L_{lob}\,\bar{Q}_{lob} + L_{ch}\,\bar{Q}_{ch} + L_{rob}\,\bar{Q}_{rob}}{\bar{Q}_{lob} + \bar{Q}_{ch} + \bar{Q}_{rob}} \qquad (eq. 16)$$

| | |
|---|---|
| $L_{lob}$ , $L_{ch}$ , $L_{rob}$ | cross section reach lengths specified for flow in the left overbank, main channel, and right overbank, respectively |
| $\bar{Q}_{lob}$, $\bar{Q}_{ch}$, $\bar{Q}_{rob}$ | arithmetic average of the flows between sections for the left overbank, main channel, and right overbank, respectively |

The representative friction slope $\bar{S_f}$ calculated as shown below in the average convergence equation (equation 17).

$$\bar{S}_f = \left(\frac{Q_1 + Q_2}{K_1 + K_2}\right)^2 \qquad (eq. 17)$$

| | |
|---|---|
| $Q_1, Q_2$ | Discharge in two cross sections |
| $K_1, K_2$ | Conveyance for the cross sections. |

Cross section conveyance can be calculated generally as follow in (equation 18).

$$K = \frac{1}{n} AR^{2/3} \qquad (eq. 18)$$

| | |
|---|---|
| $n$ | manning's coefficient of roughness |
| $A$ | flow area cross section |
| $R$ | Hydraulic radius |

Finally, the continuity equation (equation 19) is also used to solve the velocity and water surface profile. It produces the same flow in the channel as it contracts or expands.

$$Q = A_1V_1 = A_2V_2 \qquad (eq. 19)$$

| | |
|---|---|
| $Q$ | River discharge |
| $A_1, A_2$ | Cross sectioanla area at two points |
| $V_1, V_2$ | Discharge velocity at two points |

## 4.3 Bridges

The bridges influence the flow of water by enforcing the passage of the water through a narrower channel. It may increase the water level and, for example, change the velocity of a critical section of the river. It is essential that the placement of cross sections within the structure is considered so that HEC RAS can perform the calculations in the most effective manner. As part of the procedure, place cross-sections, define ineffective flow areas, insert bridge geometry, and evaluate energy losses around bridges. An example of a basic cross-section plan layout with four cross-sections can be seen in Figure 19. In HEC RAS, energy losses are calculated based on three zones. Moreover, HEC RAS uses different methods to calculate energy loss at bridges depending on the characteristics of the flow.

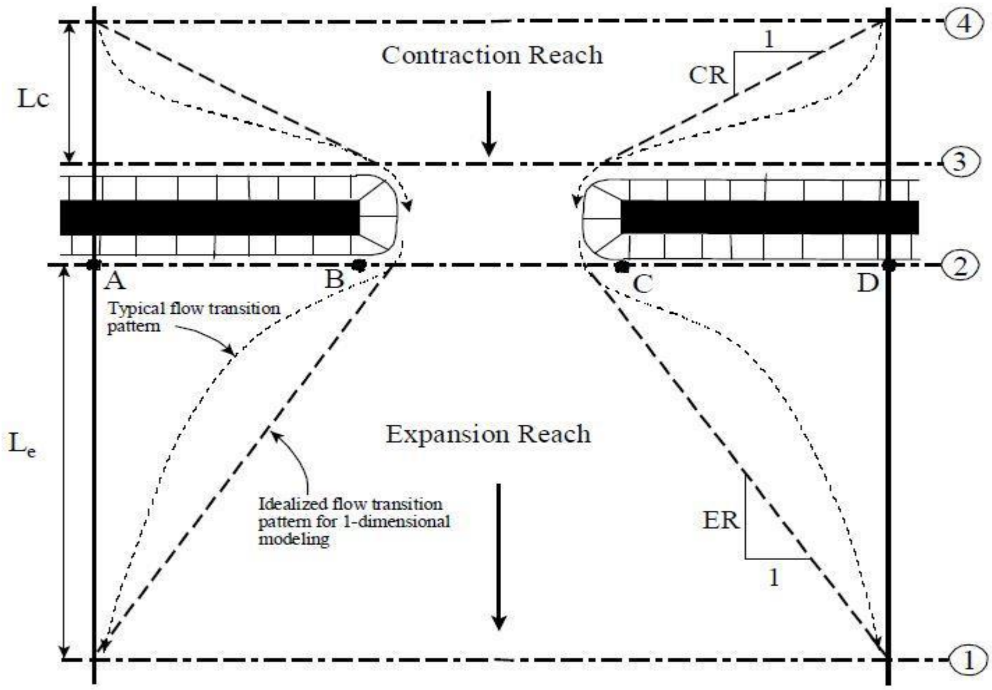


Figure 19. *Bridge cross section layout* (Brunner, 2021).

***Zone 1***

As a result of an expansion of the flow downstream of the bridge (cross-sections 2 to 1), energy is lost immediately downstream of the bridge. These losses are calculated as friction and expansion losses; the equations are presented above.

***Zone 2***

In the region immediately upstream of the bridge (cross-sections 4 to 3), energy is lost due to friction and contraction losses; the equations listed above are used to calculate this energy loss.

***Zone 3***

Four different approaches (Energy Equation, Momentum Balance Method, Yarnell Equation, and FHWA WSPRO Method) can be used to calculate the energy loss at the bridge structure (cross-sections 3 to 2).

## 4.4 Dams / Gates

Modeling of inline structures is possible with HEC RAS, such as gated spillways, overflow weirs, drop structures, as well as lateral structures. A radial gate can be modeled with HEC RAS, as well as a vertical lift gate (such as a sluice gate) and an overflow gate. Depending on the type of spillway crest, either an ogee or a broad crested weir can be described. Furthermore, a separate uncontrolled overflow weir can be defined in addition to gate openings; see Figure 20 below (Brunner, 2021).

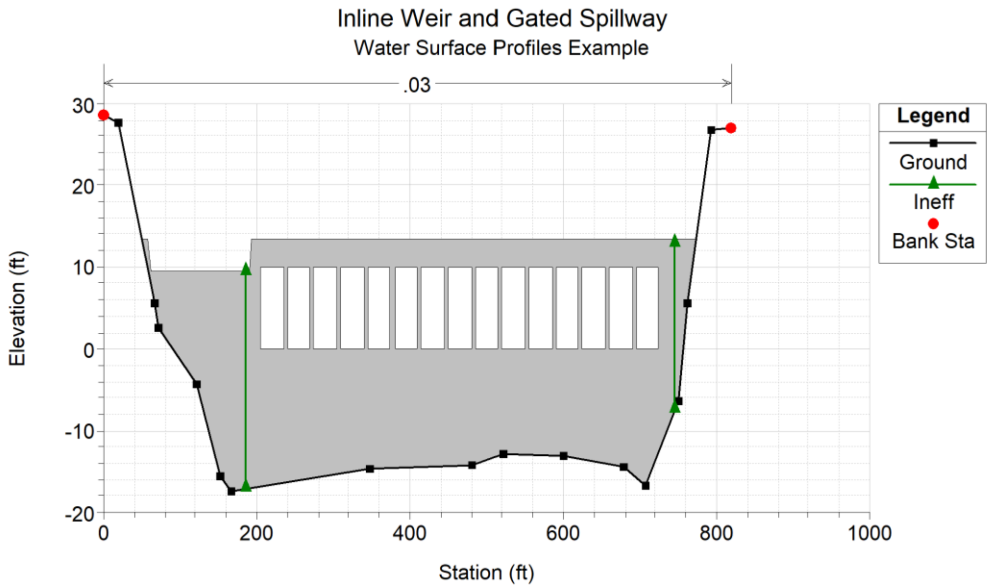


Figure 20. *The embankment is specified as an overflow weir over the entire top of the embankment and there are 15 identical gate openings.* (Brunner, 2021).

## 4.5 Boundary Conditions

The boundary conditions must be set for steady flow to enable the program to determine the water surface conditions and begin the calculation. Flow modes of rivers can include the following:

- The subcritical flow regime
- The supercritical flow regime
- The mixed flow regime

Flow regimes under subcritical conditions require boundary conditions at the downstream end, whereas flow regimes under supercritical conditions require boundary conditions only at the upstream end. An upstream and downstream boundary condition are required in a mixed flow regime. In order to simulate steady flow with HEC RAS, the following boundary conditions may be used:

- Rating curve
- Known water surface level
- Critical depth
- Normal depth

## 4.6 Flood Hazards Mapping

Flood hazard maps provide graphic evidence of flooding (predicted areas of flooding, depth of flooding, etc.), in an easy-to-understand manner. It illustrates flood hazard areas and enables administrators and planners to identify areas of risk, prioritize mitigation and response efforts, and facilitate the identification of flood hazards (Ghosh and Silva, 2018). In terms of damage, floods are the most frequent and damaging disasters in the world (Duan et al., 2012). Furthermore, the force generated by deeper, faster flows can cause more damage than the force produced by shallow, slow flows (Water Research Laboratory, 2015).

HEC RAS provides the ability to create flood hazard maps after running the model through its Raster Calculator function. This can be accomplished by creating a New Results Map Layer based on Depth*Velocity. Figure 21 can be used as a basis for classifying flood hazards; this method described by Smith, Davey, and Cox (2014). In the case of water depths exceeding 2m, even a low water velocity of 0.5 m/s is unsafe for a structure. Similarly, a flow with a velocity of more than 2 m/s is unsafe for a structure with a depth of 0.5 m; therefore, special engineering consideration must be taken in order to design buildings or structures in these cases. Furthermore, all building types are considered vulnerable to failure when the flow depth or velocity exceeds 4m or 4m/s, respectively.

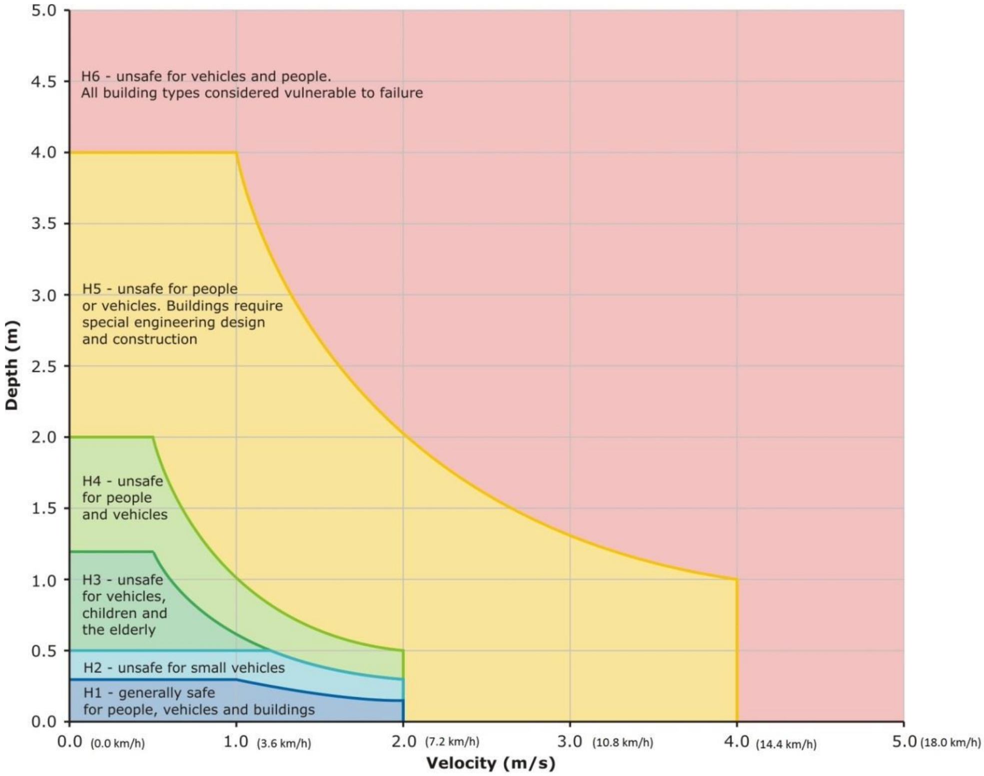

Figure 21. *Vulnerability curves for flood hazards* (Smith et al., 2014).

## 4.7 Local Scour Calculations for Abutments in HEC RAS

Bridge abutments are located at both ends of the bridge and act as a means of transmitting the bridge's weight, including traffic, to the foundation (Das et al., 2021). When abutments obstruct flow, local scour occurs. By blocking the flow, a horizontal vortex is generated starting at the upstream end of the abutment and running along the abutment's toe, followed by a vertical wake vortex at its downstream end.

Based on the recommendations made in the HEC 18 report, two equations are presented for the calculation of the live-bed abutment scour. The HEC 18 report recommends the use of the HIRE equation when the wetted embankment length ($L$) is greater than 25 times of the approach flow depth

($y_1$). If the wet embankment length is less or equal to 25 when divided by the approach depth, the HEC 18 report suggests using the Froehlich equation (Froehlich, 1989). A description of the equations is provided in section 2.7.1.

In HEC RAS, the HEC 18 method of bridge scour analysis is integrated (Das et al., 2021). HEC RAS calculates the abutment scour separately for the left and right abutments. It is not necessary for the user to enter any additional details other than the type of abutment (spill-through, vertical, vertical with wing walls). Based on the hydraulic output and default settings, the program automatically selects the values for all other variables. In spite of this, the user has the option to change any variable. As the roadway embankment intersects the natural ground, the location of the toe of the abutment is determined. The cross-section stationing is very important in the context of abutment scour calculations since the hydraulic variables would be derived from the output of the flow distribution at this cross-section stationing. In the event that the user is not satisfied with the stationing that is selected by the model, they have the option to override it by entering their own (CEIWR-HEC, 2021).

## 4.8 Bridge Scour Analysis Limitations in HEC RAS

Bridge scour analysis conducted by the HEC RAS conforms to all the limitations outlined in the HEC 18 manual. Therefore, it is more reasonable to use it for uniform, non-stratified, and non-cohesive beds. The actual conditions, though, are often more complex. It should also be noted that the hydraulic characteristics underlying the equations for scour depth are derived from a 1D hydraulic model in which steady flow conditions prevail. Due to roughness patterns and obstructions, however, the distribution of flow is unsteady for realistic bridge cross sections. In evaluating the HEC RAS model predictions, it is also critical to consider the degree of uncertainty in the empirical equations. By using HEC RAS analysis, it is not possible to analyze scour depth over time or to predict scour rate over time (Inamdeen, 2020).

# 5 Model Implementation

## 5.1 Digital Elevation Model (DEM) and Bathymetry

The terrain data (topographic and bathymetric) is one of the most important elements of a hydraulic model. In order to conduct this study, data from Swedish authorities were obtained. The DEM in TIF format and SWEREF 99 projection were downloaded using the Geographic Extraction Tool. This tool is available for research and educational purposes from the Centre for Geographical Information Systems at Lund University. The data is compiled from the following sources:

- Lantmäteriet (Swedish Surveying and Cadastral Agency),
- Sveriges geologiska undersökning, SGU (Sweden Geological Survey),
- Statistiska centralbyrån, SCB (Statistics Sweden),
- Sjöfartsverket (Swedish Maritime Administration).

However, the elevation data are available only above water surface; therefore, the bathymetric data with a 0.5 m resolution was obtained from Ljungby Municipality for the study area also in TIF format and SWEREF 99 projection. Later, these two raster files were merged using Arc GIS Pro to have accurate topography and bathymetry for the study area to create a center line for the river, bank lines, flow path, and cross sections. Raster files also can be merged in HEC RAS while creating a New Terrain Layer in RAS Mapper. Finally, the raster files were also visualized in SCALGO Live Tool as shown in Figure 22.

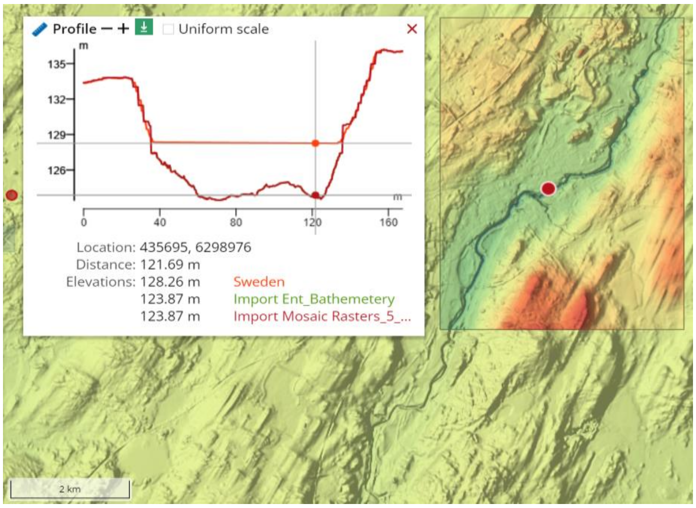


Figure 22. *Shows the study area with DEM and bathymetry rasters; a distinct difference in elevation can be observed.*

## 5.2 Structures Details (Bridges & Dam)

As mentioned, there are ten bridges over the Lagan River in Ljungby Municipality and one hydropower dam. The first bridge in upstream (Sickingebron) belongs to the Swedish Transport Administration (Trafikverket), and the drawing details can be found in the bridge and tunnel management system (BaTMan) for authorized users. The rest of the bridges belong to the municipality. Thus, the municipality provided drawings for six of them of varying date. These drawing details are needed to define the top elevation of the bridge, opening for the bridges, the elevation of the lower chord, the width of the road, and pier dimensions and locations. Drawings of three bridges (Replösabron, Ljungsatersbron, and Söderbron), as well as the hydropower dam, were not available. SCALGO Live was used to find the top elevation of the bridges and the dam, the opening distance measured on RAS Mapper, and some pictures on the municipality website were reviewed to derive the inputs to the HEC RAS model.

## 5.3 Manning's Number

The Manning's coefficient "n" represents the roughness of a channel surface compared to its flow direction. In most cases, the value is derived from reference tables, such as those presented by Chow (1959), but measurements obtained from the field can also be used. Manning's coefficient can have a significant impact on the results of a model and should be selected appropriately (Sukupayo, 2021; CEIWR-HEC, 2021). In this model, Manning's n values were initially set to 0.06, 0.035, 0.06 for Left OverBank (LOB), Main Channel, and Right OverBank (ROB), respectively, according to the Chow reference table. For calibration purposes, these values can be modified, and the validation should be done using the same calibrated parameter values. Figure 23 illustrates a cross section with Manning's n values.

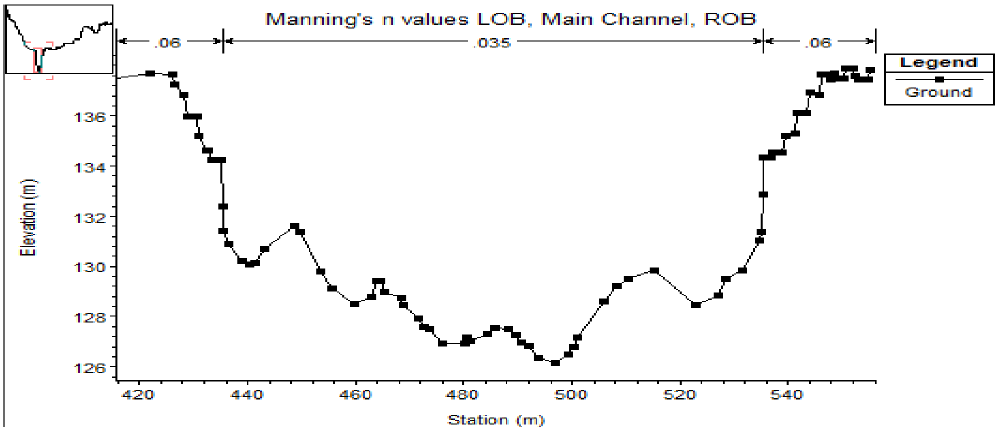


Figure 23. *A cross section with Manning's n values in the LOB, Main Channel, and ROB*.

## 5.4 Boundary Conditions

The initial water surface elevation of a river system is determined at boundary conditions. In order to perform mixed flow regime analysis, each end of the river system must have boundary conditions.

Normal depth is selected as the upstream boundary condition in this study. The user must enter an energy slope to calculate normal depth (from Manning's equation). The energy slope could be approximated by entering either the surface slope of the water or the channel bottom slope. In our case, we found the bottom slope of the channel through the river bathymetry layer (normal slope S = 0.0012).

A rating Curve is defined as the downstream boundary condition. When this type of boundary condition is selected, it is necessary to enter an elevation versus flow rating curve as shown in Figure 24. For this study the downstream boundary condition is fixed using a rating curve at the lower boundary. In order to determine the rating curve, water levels at the most downstream point were adjusted for corresponding daily river flows of the river. These flows correlate with the average daily water levels at the water level measuring station. The correlation was obtained for the first twelve values after running a large number of HEC RAS simulations to fine-tune the model. However, the last two values (13 and 14) are extrapolated from the first twelve values and correspond to 100 year and 200 year events, respectively. Without adding these values, HEC RAS will only extrapolate the last two values to determine water levels for the 100 year and 200 year events.

HEC-RAS

Enter/Edit rating curve for downstream of reach:
Reach 1

| | Stage (m) | Flow (m3/s) |
|---|---|---|
| 1 | 128 | 6 |
| 2 | 128.12 | 6.4 |
| 3 | 128.31 | 10 |
| 4 | 128.62 | 20 |
| 5 | 128.9 | 39.9 |
| 6 | 129.84 | 60 |
| 7 | 130.39 | 80.7 |
| 8 | 131.3 | 101.5 |
| 9 | 131.87 | 134.9 |
| 10 | 131.88 | 135 |
| 11 | 132 | 140 |
| 12 | 132.4 | 145 |
| 13 | 132.98 | 168 |
| 14 | 133.25 | 177 |

OK Cancel

Figure 24. *Elevation versus flow rating curve, used as downstream boundary condition in this study.*

## 5.5 Extreme Floods

### 5.5.1 Floods and return periods

The return period is often used as a measure for the risk of flooding and it describes the average time between two floods of the same extent. However, the concept of return record gives a false sense of security, as it indicates the probability for a single year and not the total probability for a period of several years (MSB – Myndigheten för samhällsskydd och beredskap, The Swedish Civil Contingencies Agency, 2020). See Table 4 below.

| *Flood Event* | *Probability of Accurance (%) In a Certain Period (Y)* | | | | | |
|---|---|---|---|---|---|---|
| | *10 Y* | *50 Y* | *100 Y* | *200 Y* | *500 Y* | *1 000 Y* |
| *20-years Event* | 40 | 92 | 99 | 100 | 100 | 100 |
| *50-years Event* | 18 | 64 | 87 | 98 | 100 | 100 |
| *100-years Event* | 10 | 40 | 63 | 87 | 99 | 100 |
| *200-years Event* | 5 | 22 | 39 | 63 | 92 | 99 |
| *1 000-years Event* | 1 | 5 | 10 | 18 | 39 | 63 |
| *10 000-years Event* | 0.1 | 0.5 | 1 | 2 | 5 | 9.5 |

Table 4 *The total probability that a flow with a certain return time will be exceeded over a longer period of time. For example, a flow with a return period of 100 years has a 40% probability of occurring over a 50-year period and a flow with a return period of 10,000 years has a 1% probability of occurring over a 100-year period* (MSB, 2020).

It is difficult to calculate floods with very long return periods (1,000 years or more) using a short period of available data; this creates a great deal of uncertainty. Normally, there are less than 100 years of observations to start from and in regulated systems, the observed water flow series are significantly shorter.

### 5.5.2 Climate Change Influence

As a result of climate change, the frequency of floods is expected to increase in Sweden in the future. Nordic countries are will most likely to experience a greater rise in temperatures than the global average. Rainfall is projected to increase primarily in the north and in the southwest of the country, while drought can be expected in the southeast. Temperature and precipitation changes are predicted to affect runoff into waterways (Ek et al., 2016).

The return periods for floods that occur every 20 and 50 years have been observed to decrease in the temperate climate zones including Western Europe. As a result of this climatological change, floods that had a return period of 20 and 50 years in 1970 have now a return period of 8 and 21 years, respectively, in temperate climates throughout the world (Slater et al., 2021).

### 5.5.3 Flood Frequency Analysis (FFA)

Flood frequency analysis determines how often a certain flow will occur. In order to calculate the hydraulic conditions in a river, such an estimation is required. This analysis may be conducted by fitting a probability model to the sample of annual extreme flood values collected from the Swedish Meteorological and Hydrological Institute (SMHI) for the Lagan River over the last 40 years (1981-2020). In this way, it will be possible to determine the recurrence intervals for extreme events (Pegram and Parak, 2004). This study will analyze flood frequency using the RMC-BestFit software and apply the generalized extreme value distribution (GEV).

***RMC-BestFit Software***

As part of its Risk Management Center (RMC), the U.S. Army Corps of Engineers (USACE) has developed Bayesian estimation and fitting software (RMC-BestFit) for flood hazard assessments in communities of practice such as flood risk management, planning, and dams and levees.

In RMC-BestFit, thirteen probability distributions are selected to fit distributions and to perform Bayesian estimation. This software provides a fully integrated modeling platform that includes a modern graphical user interface, data entry capability, analysis capability for fitting distributions, Bayesian estimation analysis, and quality reports (RMC-BestFit, 2022).

### *Generalized Extreme Value Distribution (GEV)*

Generalized extreme value distribution is used in many fields, including for hydrologic frequency analysis, insurance, and risk management. The GEV distribution has three parameters, location ($\xi$), scale ($\alpha$), and shape ($\kappa$), encompassing the following distributions: Gumbel (EVI), Fréchet (EVII), and Weibull (EVIII). Depending on the shape parameter $\kappa$, the GEV may represent one of the three sub-distributions (RMC-BestFit, 2022). Equation 20 shows the GEV distribution function. In view of the obtained parameters, as shown below, the distribution in the present case is a Gumbel or type I extreme value distribution, since the $\kappa$ value is almost zero. The frequency plot in Figure 25 shows the annual exceedance probability with respect to the GEV distribution, from where the Lagan river extreme flow values were obtained.

$$\begin{cases} Z = -\frac{1}{k}\ln\left(1 - k\left(\frac{x-\xi}{\alpha}\right)\right) & if\ k \neq 0, \\ Z = \left(\frac{x-\xi}{\alpha}\right) & if\ k = 0. \end{cases} \qquad (eq.20)$$

| Parameter | Value |
|---|---|
| $\xi$ | 78.06 |
| $\alpha$ | 16.67 |
| **$\kappa$** | **0.11** |

Table 5. *The obtained distribution is a Gumbel or type I distribution since κ has almost a zero value.*

.

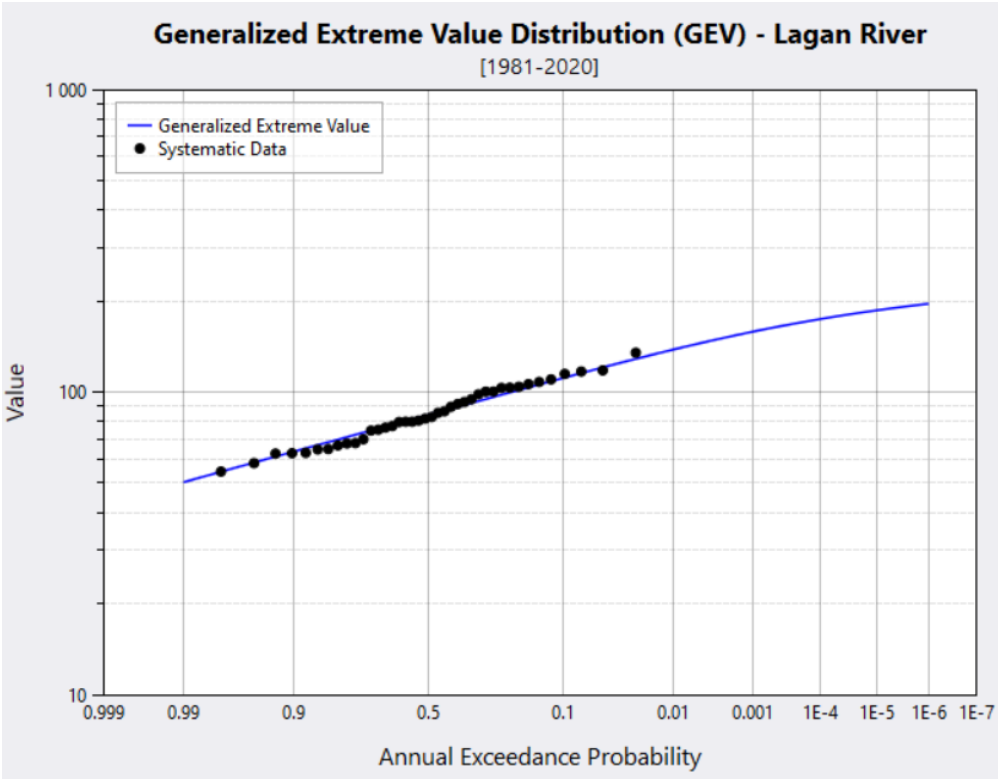


Figure 25. *Flood frequency analysis for Lagan River extreme flows and a fit with a generalized extreme value distribution (GEV) [1981-2020].*

# 6 Model Simulation

## 6.1 Calibration and Validation

The main objective of this study is to determine the impact of overflowing on bridges, so water surface elevation (WSE) data from a monitoring station were used to calibrate and validate the model after creating the hydraulic model; the location can be seen in Figure 26. In order to calibrate and validate the model, data from Ljungby Municipality were provided encompassing hourly records of WSE for the period 01-June-2018 to 12-April-2021 (1047 days). Approximately 60% of the records were used for calibration, while 40% are used for validation. In February 2020, a 25 year event took place; this value was used as an input flow for the scenario of a 25 year event (Q25), which will be discussed later.


Figure 26. *Water elevation station located in Ljungby.*

For model calibration, WSE data from 01-June-2018 to 31-Jan-2020 were used and compared to the simulated water level at the cross section where the water level monitoring station is located, as shown in Figure 27. The coefficient of determination ($R^2$) for the calibration was 0.87, which indicates satisfactory accuracy (See Figure 28).

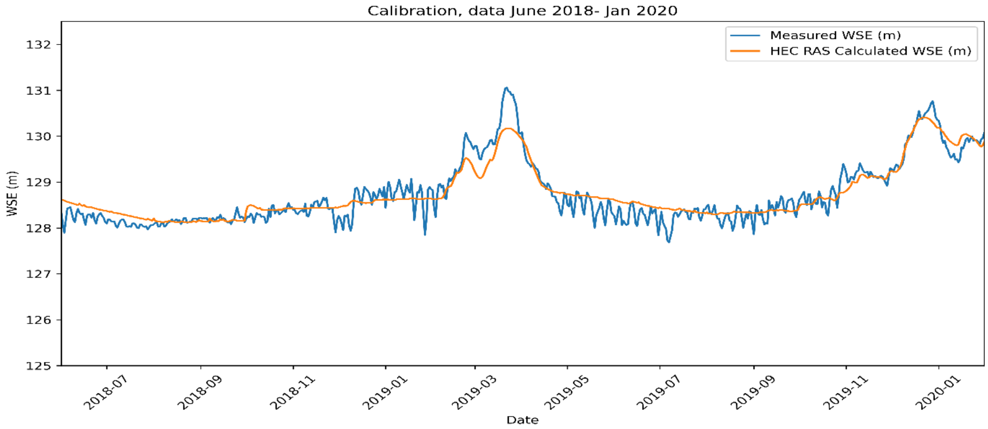


Figure 27. *Calibrated and measured water surface elevation (WSE).*

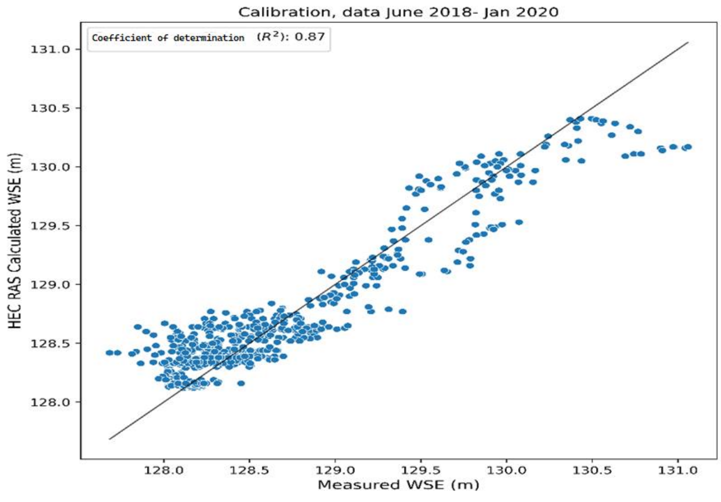


Figure 28. *Agreement between model simulation and measurement.*

For validation, WSE data from 01-Feb-2020 to 12-April-2021 were used and compared to the simulated water levels at the cross section where the water level monitoring station is located, Figure 29. The coefficient of determination ($R^2$) for the validation was 0.90, which again indicates satisfactory accuracy (See Figure 30).

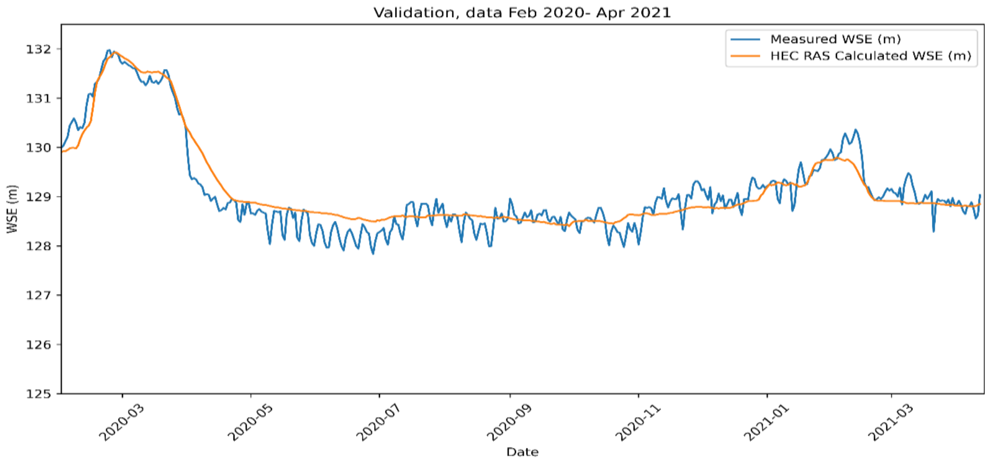


Figure 29. *Validated and measured water surface elevation (WSE)*

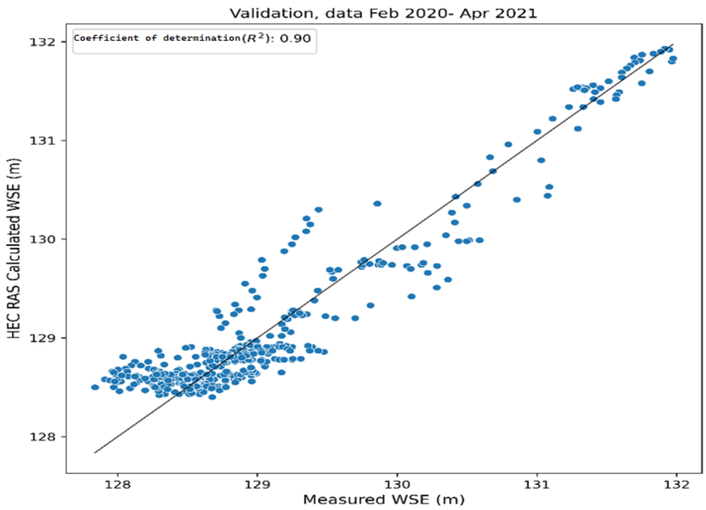


Figure 30. *Coefficient of determination for model validation.*

## 6.2 Simulation Scenarios

Three scenarios were simulated with the model: a 25-year event (Q25), a 100-year event (Q100), and a 200-year event (Q200) for mapping flood hazards. These flow values were derived using the FFA, as described in the previous section (Table 6 indicates which flow values were used as inputs for the model in each scenario). Subsequently, the Q100 and Q200 simulation results were used to estimate the scour on bridges abutments. In Figure 31, the Ljungsätersbron bridge is shown out of service during an observed 25-year event flow (Jonsson, 2020).

Figure 31. *A 25-year event in Lagan River at Ljungby; the Ljungsätersbron bridge is shown to be out of service* (Jonsson, 2020).

| *Simulated Event* | *Estimated Flow $Q_{est}$ ($m^3/s$)* |
|---|---|
| *25-year Event* (Q25) | 139 |
| *100-year Event* (Q100) | 168 |
| *200-year Event* (Q200) | 177 |

Table 6. *Flow values, used as inputs for the model simulations in each scenario.*

# 7 Results and Discussion

Flood hazard maps for all three scenarios are presented and discussed in this chapter. Overflowed bridges were identified for Q100 and Q200 events in order to assess bridge scouring at abutments. The assessment of contraction and pier scour was not carried out since it is primarily dependent on sediment and riverbed materials; these data are not currently available, but this type of scour can easily be incorporated in this model, if sieve analysis is conducted in the future.

## 7.1 Flood Inundation and Hazard Maps

***Inundation map***

Natural hazards such as flooding pose a critical threat to lives, assets, and the environment. Thus, the first step in flood adaptation and mitigation is to identify flood hazards and predict flood inundations. Figure 32 shows the inundation map for Ljungby Municipality with different flow scenarios. The flow Q25 mostly runs through the main river body; however, Q100 and Q200 will inundate the southern part of the municipality. Therefore, flood control measurements are needed to avoid related risks during these events.

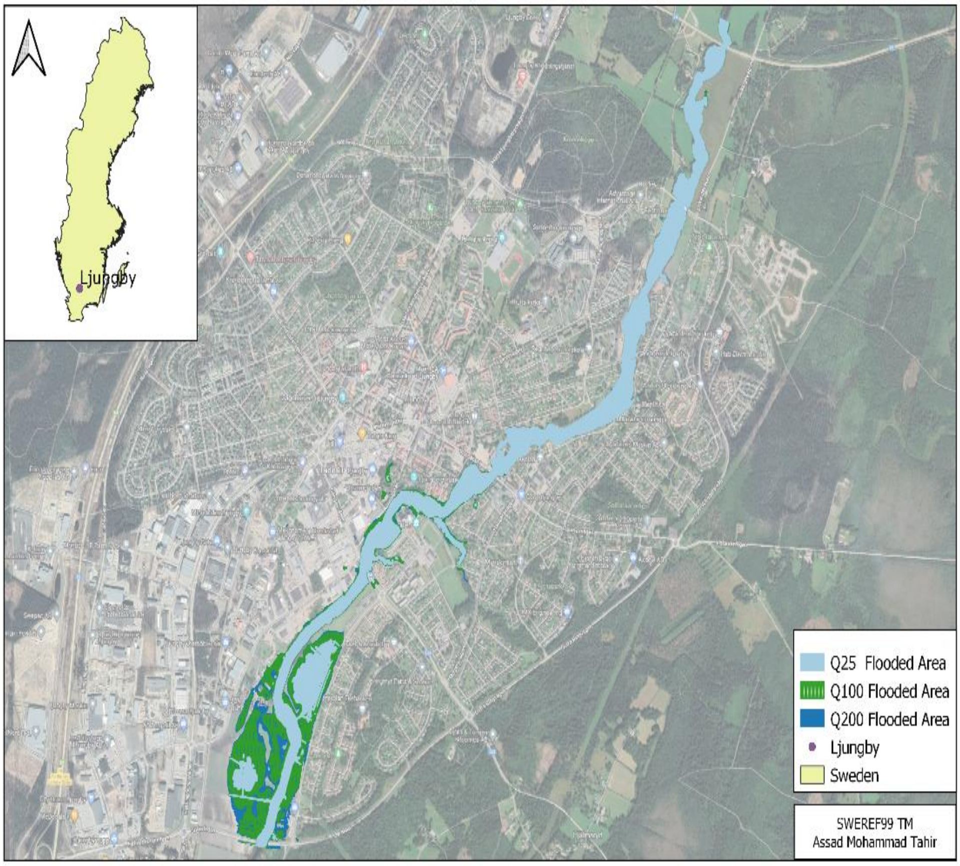


Figure 32. *An inundation map for Ljungby Municipality under the three studied flooding scenarios.*

### *Flood hazard maps*

Combined flood hazard curves (combination of velocity and depth of floodwaters combined) as shown in (Figure 21. in section 4.6) may be used to determine the level of vulnerability of a community when it encounters floodwater. Based on the combined curves, specific vulnerability thresholds are determined according to the hazard classifications specified in Table 7. The hazard maps of simulated scenarios (Q25, Q100, Q200) are shown in Figures 33, 34, and 35, respectively.

| **Flood Vulnarability Classification** | **Discription** |
|---|---|
| H6 | Unsafe for vehicles and people. All building types considered vulnerable to failure. |
| H5 | Unsafe for vehicles and people. All buildings vulnerable to structural damage. Some less robust buildings subject to failure. |
| H4 | Unsafe for vehicles and people. |
| H3 | Unsafe for vehicles. children and the elderly. |
| H2 | Unsafe for small vehicles. |
| H1 | Generally safe for vehicles, people and buildings. |

Table 7. *Description of flood hazard classification* (Smith et al., 2014).

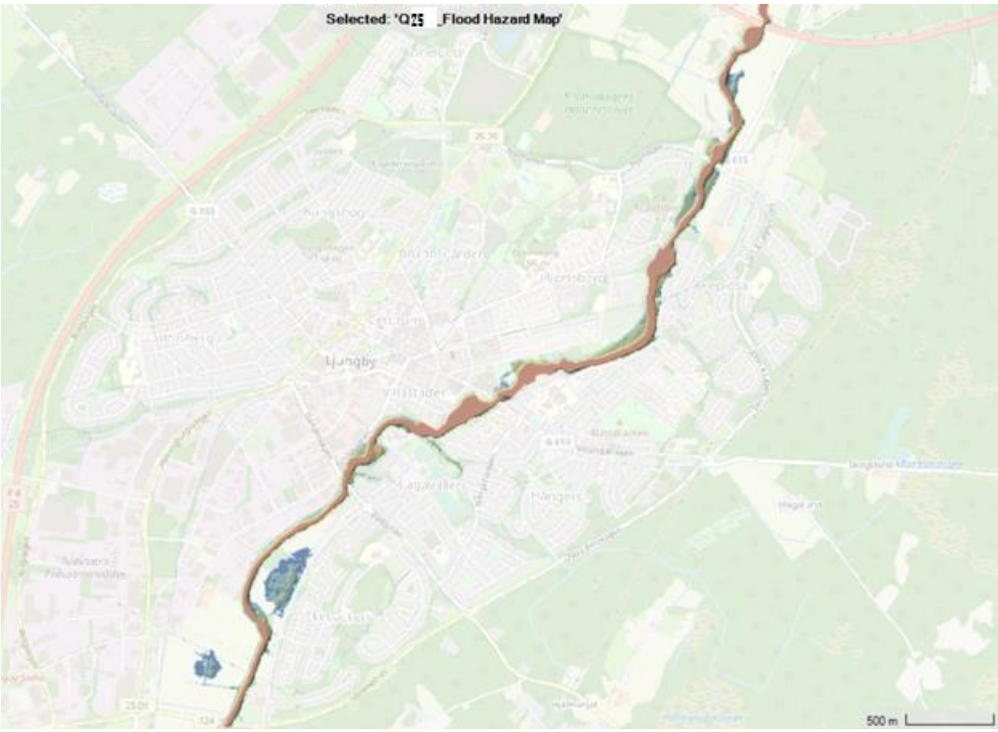


Figure 33. *Q25 flood hazard map.*


Figure 34. *Q100 flood hazard map*.


Figure 35. *Q200 flood hazard map.*

## 7.2 Overflowed Bridges and Scour Estimation

***Overflowed bridges***

The overflowing of bridges at Ljungby Municipality was estimated based on a 100 year event (Q100) and 200 year event (Q200). As a result of the flooding in Q100, Ljungsätersbron was overflowed, and water levels reached the deck of Industribron and Söderbron as well. Two river bridges were overflowed Ljungsätersbron, and Söderbron during the Q200 flood event. Additionally, the water level reached the deck of the Industribron as shown in Table 8 for Q100 and in Table 9 for Q200. A profile view shows the water surface elevation in all 3 scenarios (Q25, Q100, Q200) with bridges along the study area in Appendix III.

| *Bridge Name* | *Number in series from US to DS* | *Comment* | *Water highness above the bridge [m]* |
|---|---|---|---|
| Ljungsätersbron | 7 | Overflowed | 1.08 |
| Industribron | 8 | Water Level reached bridge’s deck | - |
| Söderbron | 10 | Water Level reached bridge’s deck | - |

Table 8. *Q100 – overflowed bridges in Ljungby Municipality.*

| *Bridge Name* | *Number in series from US to DS* | *Comment* | *Water highness above the bridge [m]* |
|---|---|---|---|
| Ljungsätersbron | 7 | Overflowed | 1.35 |
| Industribron | 8 | Water Level reached bridge’s deck | - |
| Söderbron | 10 | Overflowed | 0.25 |

Table 9. *Q200 – overflowed bridges in Ljungby Municipality.*

***Abutments scouring***

Using the Froehlich equation within the HEC RAS model with spill through abutment, the abutment scour depths were estimated for Q100 and Q200, as can be seen in Figure 36 and Table 10 below. It is important to note that the depth of abutment scour varies from bridge to bridge as a result of variations in bridge dimensions, as well as due to bathymetric and hydraulic characteristics. In addition, for the Froehlich's equation, the average depth ($y_a$) of the flow is considered as part of a safety factor. Due to this, the scour depth was manually adjusted by subtracting the average depth for each flood event.

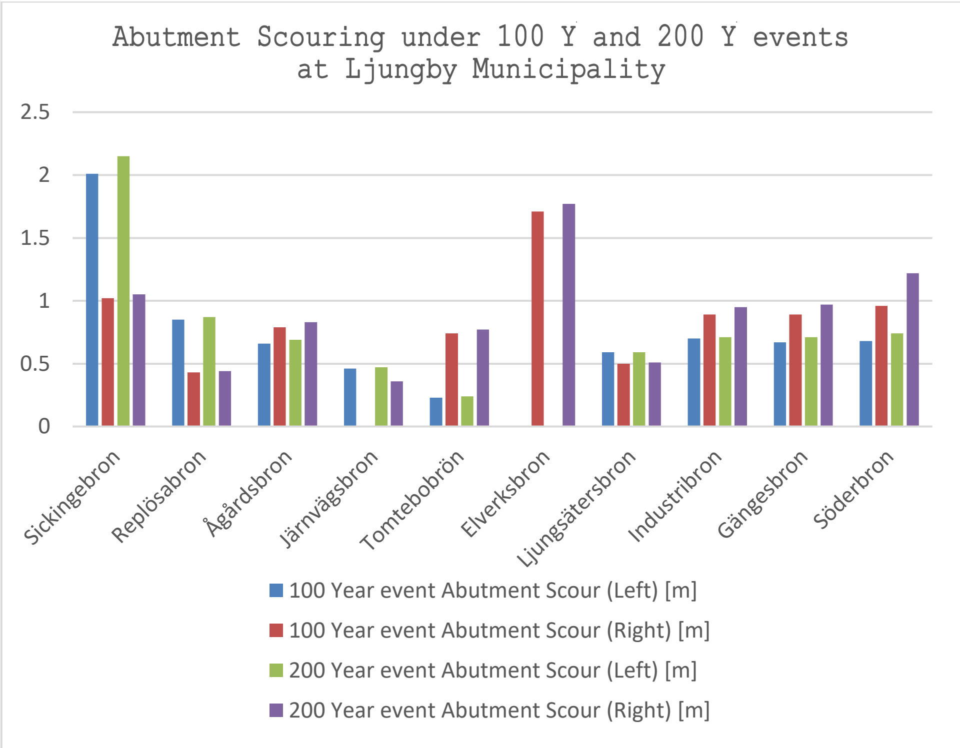


Figure 36. *A bar graph shows scour depth at all bridges at Ljungby Municipality under Q100 and Q200 events.*

| *Bridge Name* | *ID From US to DS* | *100 Year event* | | *200 Year event* | |
|---|---|---|---|---|---|
| | | *Abutment Scour* (Left) *[m]* | *Abutment Scour* (Right) *[m]* | *Abutment Scour* (Left) *[m]* | *Abutment Scour* (Right) *[m]* |
| Sickingebron | 1 | 2.01 | 1.02 | 2.15 | 1.05 |
| Replösabron | 2 | 0.85 | 0.43 | 0.87 | 0.44 |
| Ågårdsbron | 3 | 0.66 | 0.79 | 0.69 | 0.83 |
| Järnvägsbron | 4 | 0.46 | 0 | 0.47 | 0.36 |
| Tomtebobrön | 5 | 0.23 | 0.74 | 0.24 | 0.77 |
| Elverksbron | 6 | 0 | 1.71 | 0 | 1.77 |
| Ljungsätersbron | 7 | 0.59 | 0.50 | 0.59 | 0.51 |
| Industribron | 8 | 0.70 | 0.89 | 0.71 | 0.95 |
| Gängesbron | 9 | 0.67 | 0.89 | 0.71 | 0.97 |
| Söderbron | 10 | 0.68 | 0.96 | 0.74 | 1.22 |

Table 10. *Abutment scouring at all river bridges in Ljungby Municipality for the flows Q100 and Q200.*

## 7.3 Uncertainity of Results

In order to effectively evaluate the model results, it is necessary to understand the uncertainties involved. According to section 5.5.3 simulated flow data were acquired through SMHI for a period of approximately 40 years (1981-2020). In the case of events with high return periods, this could be a short period of time for frequency analysis. In the study area, there was only one water surface elevation measuring station; this is one of the reasons why we obtained a high $R^2$ for calibration and validation though this satisfies the desired results from the model. Obtaining the correct and all required dimensions from the municipal drawings for bridges was challenging. Thus, three bridge details were obtained using other tools such as SCALGO Live. It is important to note that the HEC RAS 1D model contains several governing equations based on assumptions and simplifications. Some fluid flows may have much more complex dynamic properties than what steady-state conditions describe. Another major constraint of the study was the lack of geotechnical data. Thus, it was not possible to estimate pier and contraction scouring.

# 8 Conclusion and Recommendations

This thesis focused on determining the impact of extreme river flows on bridges, specifically for river flows exceeding those specified in the designs. The design procedures in different countries, including the United States of America and Australia, have been reviewed concerning the impact of extreme flows on bridges and the problem of scouring. An analysis of the behavior of ten river bridges on the Lagan River in Ljungby has been conducted using HEC RAS. Moreover, flood hazard maps were created to determine the areas inundated and assess the risk associated with extreme flood events.

Although HEC RAS hydrodynamic (1D – Steady flow) model presented many limitations, it was reliable and robust for predicting the hydraulic behavior of the river. For the various flows within the study river reach, the HEC RAS model satisfactorily simulated the water levels; therefore, the model simulations may provide satisfactory initial estimation of local scour at bridge abutments and inundation.

As a result of the HEC RAS model, Ljungsätersbron would be overflowed in an event with a 100 year return period; also, the water level reached the bridge deck at Industribron and Söderbron as well. Two river bridges were overflowed, that is, Ljungsätersbron, and Söderbron during a 200 year event. Additionally, the water level reached the Industribron bridge deck during this event. All bridges are subjected to abutment scouring, and the depth of scouring varies from one bridge to another as a result of variations in bridge dimensions, and in bathymetric and hydraulic characteristics.

In conclusion, it is surmised that the results provide a fair estimate of the potential threats to bridge structures, as well as initial suggestions for future research. Model simulations may also be used to assess the impact of climate change on the flow of water.

***Recommendations***

- Sediment analysis of the riverbed would be beneficial along the studied river reach. In particular including the locations of bridges and locations of identified scour holes to estimate the total scouring at bridges; such data will make it possible to include contraction and pier scouring.

- In order to improve the model estimation of overflowed bridges, it will be useful to introduce several water level measuring stations in the study area, as well as obtaining more detailed drawings of the structures.

- Using the output of this model in future studies can assist in performing hydrodynamic force analyses. These analyses can help in determining whether any river bridges are at risk of collapsing due to overturning or drag and lift forces.

# References

Arneson, L., Zevenbergen, L., Lagasse, P., and Clopper, P. 2012. *Evaluating scour at bridges*. Publication No. FHWA-HIF-12-003, Hydraulic Engineering Circular No. 18, U.S. Department of Transportation, Federal Highway Administration, United States.

Australian Rainfall & Ruoff (ARR). 2019. Book 6: *Flood Hydraulics Chapter 7*: Safety Design Criteria.

Austroads (2019), *Guide to Bridge Technology Part 8: Hydraulic Design of Waterway Structures*, prepared by Hanson Ngo, Project Managers: Phanta Khamphounvong and Henry Luczak, Sydney, NSW, Australia.

Bjerkén, A. and M Persson, K., 2021. *Evaluating GIS based water budget components applicability and availability for the Lagan River catchment*. VATTEN, [online] 4, pp.229-238. Available at: <https://www.tidskriftenvatten.se/tsv-artikel/evaluating-gis-based-water-budget-components-applicability-and-availability-for-the-lagan-river-catchment/> [Accessed 4 August 2022].

Breusers, H. N. C., Nicollet, G., and Shen, H. W. 1977. *Local scour around cylindrical piers*. Journal of Hydraulic Research, 15, 211-252.

Briaud, J., Chen, H., Chang, K., Oh, S., Chen, S., Wang, J., Li, Y., Kwak, K., Nartjaho, P. and Gudaralli, R. 2011. *The SRICOS–EFA Method, Summary Report*, Texas A&M University, United States.

Brunner, G. W. (2021). *HEC-RAS River Analysis System: User's Manual*, Version 6.1, US Army Corps of Engineers, Institute for Water Resources, Hydrologic Engineering Center.

CEIWR-HEC, 2021. *HEC-RAS River Analysis System User's Manual Version 6.0*.

Chow, 1959. *Manning's n for channels*. [online] Fsl.orst.edu. Available at: <http://www.fsl.orst.edu/geowater/FX3/help/FX3_Help.html#8_Hydraulic_Reference/Mannings_n_Tables.htm> [Accessed 12 August 2022].

Chow, V.T. (1959) *Open-channel Hydraulics*, McGraw-Hill, New York.

Das, R., Inamdeen, F. and Larson, M., 2021. *Bridge Scour : Basic Mechanisms and Predictive Formulas*. [online] Lund: Lund University. Available at: <https://lup.lub.lu.se/record/0c01ac44-d63b-4af1-9d7d-6e24abc1b254> [Accessed 3 August 2022].

Duan, M., Zhang, J., Liu, Z. and Aekakkararungroj, A., 2012. *USE OF REMOTE SENSING AND GIS FOR FLOOD HAZARD MAPPING IN CHIANG MAI PROVINCE, NORTHERN THAILAND*. [online] Available at: <http://file:///C:/Users/assad/Downloads/USE_OF_REMOTE_SENSING_AND_GIS_FOR_FLOOD_HAZARD_MAP.pdf> [Accessed 8 August 2022].

Ek, K., Goytia, S., Pettersson, M. and Spegel, E., 2016. *Analysing and evaluating flood risk governance in Sweden : Adaptation to Climate Change?*. [online] DIVA. Available at: <http://ltu.diva-portal.org/smash/record.jsf?faces-redirect=true&aq2=%5B%5B%5D%5D&af=%5B%5D&searchType=SIMPLE&sortOrder2=title_sort_asc&query=&language=sv&pid=diva2%3A995169&aq=%5B%5B%5D%5D&sf=all&aqe=%5B%5D&sortOrder=author_sort_asc&onlyFullText=false&noOfRows=50&dswid=-4846> [Accessed 14 August 2022].

Froehlich, D.C., 1989. *Local Scour at Bridge Abutments, Proceedings of the 1989 National Conference on Hydraulic Engineering*, ASCE, New Orleans, LA, pp. 13-18.

Ghosh, J. and Silva, I., 2018. *Applications of geomatics in civil engineering*. Springer, pp.215-224.

Gis.lu.se. n.d. *Geodata available for Lund University*. [online] Available at: <https://www.gis.lu.se/gis-centre/geographical-data/geodata-available-lund-university> [Accessed 12 August 2022].

Gotvald, A. J., & McCallum, B. E. (2010). *Epic flooding in Georgia*. USGS Fact Sheet: 2010-3107

Haan, C.T. (1977). *Statistical Methods in Hydrology*. Iowa State University Press, Iowa.

HEC No. 18, Publication No. FHWA-IP-90-017, 3rd Edition, November 1995, Washington D.C.

Honfi, D., Williams Portal, N., Leander, J., Larsson Ivanov, O., Björnsson, Í., & Plos, M. et al. (2018). *Inspection and monitoring of bridges in Sweden*. Retrieved 22 October 2021, from http://www.diva-portal.org/smash/record.jsf?pid=diva2:1206969

Hung, C., & Yau, W. (2017). *Vulnerability evaluation of scoured bridges under floods*. Engineering Structures, 132, 288-299. doi: 10.1016/j.engstruct.2016.11.044

Huţanu, E., Mihu-Pintilie, A., Urzica, A., Paveluc, L., Stoleriu, C. and Grozavu, A., 2020. *Using 1D HEC-RAS Modeling and LiDAR Data to Improve Flood Hazard Maps Accuracy: A Case Study from Jijia Floodplain (NE Romania)*. Water, 12(6), p.1624.

Inamdeen, F. 2020. *Evaluation of local scour along Rönne å at Ängelholm. Analysis of detailed bathymetric data in combination with HEC RAS modeling*. Master Thesis, Report TVVR20/5019, Water Resources Engineering, Lund University, Lund, Sweden.

Inamdeen, F. and Larson, M., 2021. *Sediment Sampling and Analysis in Rönne å at Ängelholm*. [online] Lund: Lund University. Available at: <https://portal.research.lu.se/en/publications/sediment-sampling-and-analysis-in-r%C3%B6nne-%C3%A5-at-%C3%A4ngelholm> [Accessed 4 August 2022].

Inamdeen, F., Larson, M., Thiere, G. and Karlsson, C., 2021. *LOCAL SCOUR IN RIVERS DUE TO BRIDGES AND NATURAL FEATURES. A CASE STUDY FROM RÖNNE RIVER, SWEDEN*. VATTEN-Journal of Water Management and Research, [online] 77(3), pp.143-161. Available at: <https://www.tidskriftenvatten.se/tsv-artikel/local-scour-in-rivers-due-to-bridges-and-natural-features-a-case-study-from-ronne-river-sweden/> [Accessed 13 August 2022].

Jan-Eric Lundberg / SVT, 2020. *Unga hoppar från bro i Ljungby – kan vara livsfarligt*. [image] Available at: <https://www.svt.se/nyheter/lokalt/smaland/ljungbys-ungdomar-trotsar-lagen-och-hoppar-fran-broarna-trots-livsfara> [Accessed 22 September 2022].

Jonsson, M., 2020. *Översvämning utmed Lagaån februari 2020*. [video] Available at: <https://www.youtube.com/watch?v=QEVrVk-0lRo> [Accessed 16 August 2022].

Karlsson, M. and Gunnarsson, A., 2017. *Riskanalys vald vägsträcka*. [Handbook] Borlänge: Trafikverket. Available at: <https://trafikverket.ineko.se/Files/sv-SE/40426/Ineko.Product.RelatedFiles/2017_204_riskanalys_vald_vagstracka.pdf> [Accessed 16 October 2022].

Khadka, J. and Bhaukajee, J., 2018. *Rainfall-Runoff Simulation and Modelling Using HEC-HMS and HEC-RAS Models: Case Studies from Nepal and Sweden*. Master Thesis. Lund University.

Koçyiğit, M., Akay, H. and Yanmaz, M., 2016. *Flooding and Its Effects on River Bridges in Western Black Sea Region*. [online] Disasterengineering.com. Available at: <http://www.disasterengineering.com/tr/download/article-file/408214> [Accessed 3 August 2022].

Kvočka, D., Falconer, R., & Bray, M. (2016). *Flood hazard assessment for extreme flood events*. Natural Hazards, 84(3), 1569-1599. doi: 10.1007/s11069-016-2501-z

Laursen, E. M. 1963. Analysis of relief bridge scour. Journal of the Hydraulics Division, 89, 93–118.

Laursen, E.M. 1960. Scour at bridge crossings. Journal of the Hydraulics Division, 86, 39-54.

Lindström, G., Pers, C., Rosberg, J., Strömqvist, J. & Arheimer, B. (2010). *Development and testing of the HYPE (Hydrological Predictions for the Environment) water quality model for different spatial scales*. Hydrology Research 41.3–4, 295-319.

Ljungby Kommun. 2022. *Översiktlig planering*. [online] Available at: < https://www.ljungby.se/contentassets/bd634f46f012423ea0eabcd9a16c7add/del-3---hansyn-och-planeringsunderlag_220331.pdf > [Accessed 4 August 2022].

Main Roads Western Australia (2006) *Floodway Design Guide*, doc 6702-02-2230, issued 24/4/2006.

Md Ali, A., Solomatine, D. and Di Baldassarre, G., 2015. *Assessing the impact of different sources of topographic data on 1-D hydraulic modelling of floods*. Hydrology and Earth System Sciences, 19(1), pp.631-643.

Melville, B. W. and Coleman, S. E. 2000. *Bridge scour*. Water Resources Publication, LLC, Highlands Ranch, Colorado, United States.

MSB – Myndigheten för samhällsskydd och beredskap, The Swedish Civil Contingencies Agency, 2020. *Översvämningskartering utmed Lagan.* [online] Available at: <https://www.msb.se/siteassets/dokument/amnesomraden/skydd-mot-olyckor-och-farliga-amnen/naturolyckor-och-klimat/oversvamning/oversvamningskartering-vattendrag/lagan-karingasjon-till-fagelfors-2020.pdf> [Accessed 5 August 2022].

Nasr, A., Johansson, J., Larsson Ivanov, O., Björnsson, I. and Honfi, D., 2022. *Risk-based multi-criteria decision analysis method for considering the effects of climate change on bridges. Structure and Infrastructure Engineering*, [online] pp.1-14. Available at: <https://www.tandfonline.com/doi/full/10.1080/15732479.2022.2033278?scroll=top&needAccess=true> [Accessed 11 August 2022].

Parola, A. C., Hagerty, D. J., and Kamojjal, S. (1998). *Highway infrastructure damage caused by the 1993 upper Mississippi River basin flooding.* Report No. NCHRP-417, Transportation Research Board, Washington, DC.

Pegram, G. and Parak, M., 2004. *A review of the regional maximum flood and rational formula using geomorphological information and observed floods. Water SA*, [online] 30(3), pp.377-392. Available at: <https://www.ajol.info/index.php/wsa/article/view/5087> [Accessed 14 August 2022].

Queensland Department of Transport and Main Roads (2019), *Bridge Scour Manual, Supplement to Austroads Guide to Bridge Technology Part 8, Chapter 5: Bridge Scour* (2018), TMR, Brisbane, Queensland.

Richardson, E.V., Harrison, L.J., Richardson, J.R., and Davis, S.R. 1993. *Evaluating scour at bridges*, 2nd edition. Publication No. FHWA–IP–90–017, Hydraulic Engineering Circular No. 18, U.S. Department of Transportation, Federal Highway Administration, United States.

Risk Management Center (RMC-BestFit). 2022. [online] Available at: <https://www.rmc.usace.army.mil/Software/RMC-BestFit/> [Accessed 14 August 2022].

Siregar, R. (2018). *Hydraulic modeling of flow impact on bridge structures: a case study on Citarum bridge*. IOP Conference Series: Materials Science And Engineering, 309, 012015. doi: 10.1088/1757-899x/309/1/012015

Slater, L., Villarini, G., Archfield, S., Faulkner, D., Lamb, R., Khouakhi, A. and Yin, J., 2021. *Global Changes in 20-Year, 50-Year, and 100-Year River Floods.* Geophysical Research Letters, [online] 48(6). Available at: <https://agupubs.onlinelibrary.wiley.com/doi/epdf/10.1029/2020GL091824> [Accessed 14 October 2022].

SMHI. 2013. *HYPE: Our Hydrological Model*. [online] Available at: <https://www.smhi.se/en/research/research-departments/hydrology/hype-our-hydrological-model-1.7994> [Accessed 22 September 2022].

Smith, G.P., Davey, E.K. and Cox, R.J. (2014), Flood Hazard UNSW Australia Water Research Laboratory Technical Report 2014/07 30 September 2014.

Sukupayo, I. (2021) *Modelling of water and material transport in river storån to Lake Bolmen, Modelling of water and material transport in River Storån to Lake Bolmen*. Available at: https://lup.lub.lu.se/student-papers/search/publication/9054536 (Accessed: November 29, 2022).

Vägverket 1987. *Erosionsskydd i vatten vid väg- och brobyggnad*. Publikation 1987:18, Vägverket, Borlänge (in Swedish).

Water Research Laboratory, 2015. *Expert Opinion: Stability of People, Vehicles and Buildings in Flood Water*. [online] Available at: <https://www.granthaminquiry.qld.gov.au/assets/stability-of-people-vehicles-buildings-flood-water-grantley-smith.pdf> [Accessed 8 August 2022].

Yoon, K., Lee, S., & Hong, S. (2019). *Time-Averaged Turbulent Velocity Flow Field through the Various Bridge Contractions during Large Flooding*. Water, 11(1), 143. doi: 10.3390/w11010143

# Appendix I

Based on the following code in RASter Calculator, the flood hazard maps will be presented in a similar manner to the vulnerability curves for flooding hazards (Smith et al., 2014).
Copy line (32 – 46) to the RASter Calculator.

The Code Compiled Successfully!

```
0  Imports System
1  Imports System.Linq
2  Imports System.Collections.Generic
3
4  Namespace RasterCode
5    Public Class Processor
6      Public Shared Function ProcessTile(inputTiles As List(of Single())) As Single()
7        Const NoData As Single = -9999.0
8        Dim length As Integer = inputTiles.First().Length
9        For Each tile As Single() In inputTiles
10         If tile Is Nothing OrElse tile.Length <> length Then Throw New ArgumentException("Tile has invalid dimensions.")
11       Next
12
13       Dim returnArray(length - 1) as Single
14       For i as Integer = 0 to length - 1
15         Dim v As Single = inputTiles(0)(i)
16         Dim d As Single = inputTiles(1)(i)
17         Dim Output As Single = NoData
18
19 ' #BEGINSCRIPT:
20
21 ‘————————————————————————————-
22 ‘ rasscript for Flood Hazard mapping based on
23 ‘ WRL Technical Report 2014/07 Flood Hazard
24 ‘ by G P Smith, E K Davey and R J Cox
25 ‘ UNSW Water Research Laboratory
26 ‘ https://knowledge.aidr.org.au/media/2334/wrl-flood-hazard-techinical-report-september-2014.pdf
27 ‘ As cited in ARR 2019 Book 6: Flood Hydraulics Chapter 7: Safety Design Criteria
28 ‘ http://book.arr.org.au.s3-website-ap-southeast-2.amazonaws.com/
29 ‘ Figure 5-5 and Table 5-2
30 ‘ Requirements: Terrain, Depth, ‘d’ and Velocity, ‘v’
31 ‘————————————————————————————-
32 If d = NoData OrElse v = NoData Then
33 Output = NoData
34 ElseIf d > 4 Or v > 4 Or d*v > 4 Then
35 Output = 6 ‘H6 unsafe for people, vehicles  all buildings
36 ElseIf d > 2 Or v>2 Or d*v>1 Then
37 Output = 5 ‘H5 unsafe for people, vehicles  some buildings
38 ElseIf d > 1.2 Or d * v > 0.6 Then
39 Output = 4 ‘H4 unsafe for people  vehicle
40 ElseIf d > 0.5 Then
```

```
Output = 3 ‘H3 unsafe for vehicle and vulnerable people
ElseIf d > 0.3 Or d * v > 0.3 Then
Output = 2 ‘H2 unsafe for small vehicles
Else
Output = 1 ‘H1 generally safe for people, vehicles,  buildings
End If

' #ENDSCRIPT:

        returnArray(i) = Output
      Next

      return returnArray
    End Function
  End Class
End Namespace

' #VARIABLE: v = 2903_SF_Mix_2_100Y | velocity | 0 | Fixed Profile
' #VARIABLE: d = 2903_SF_Mix_2_100Y | depth | 0 | Fixed Profile
```

# Appendix II

Example of an engineering drawing of one of the river bridges at Ljungby Municipality.

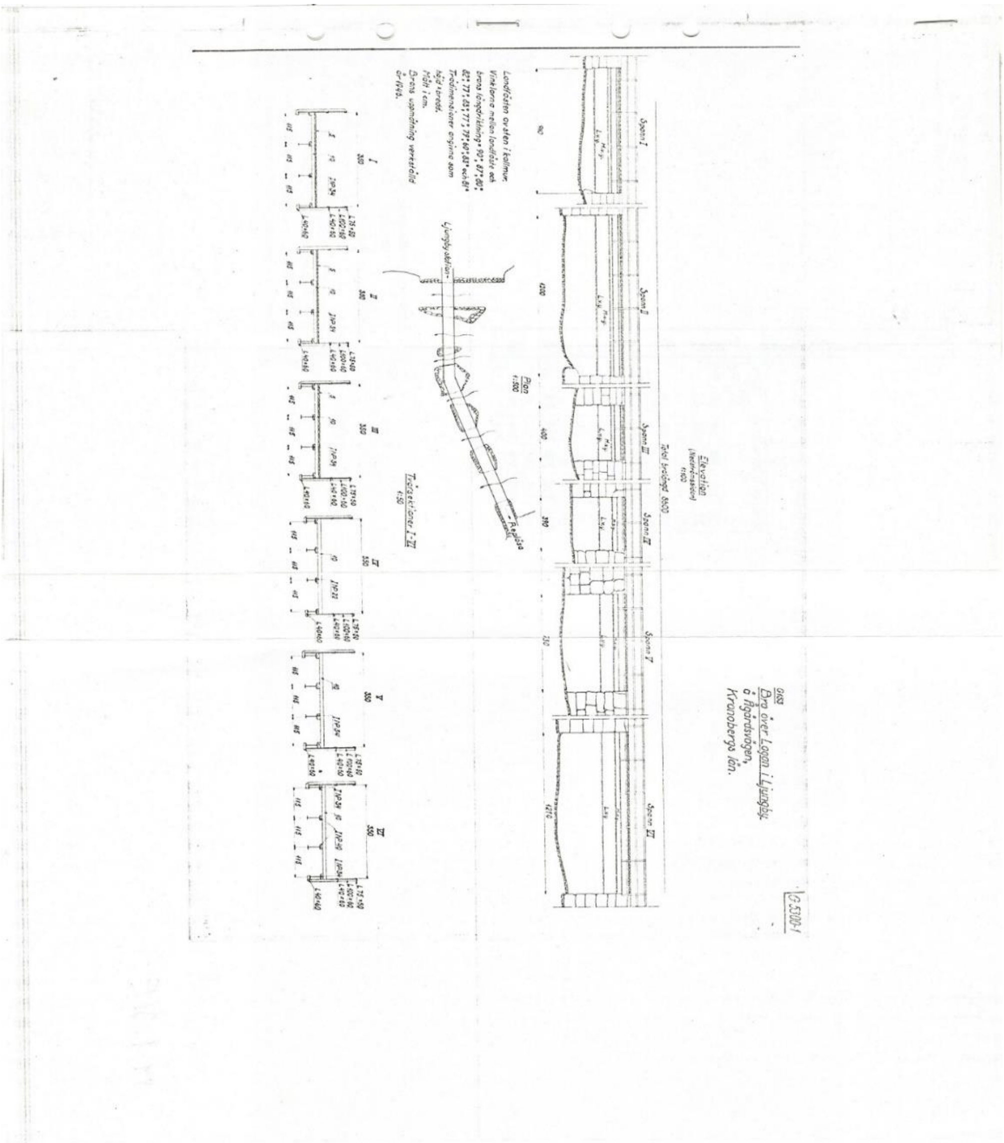

# Appendix III

A profile shows the water surface elevation for all 3 scenarios (Q25, Q100, Q200) with the bridges along the study area.